Three Dimensional Numerical Analysis of Composite Ground Improved by Deep Mixing Method

OUTLINE

- **Introduction**
- **Literature Review**
- **Methodology**

  (1) Data Collection

  (2) Numerical Analysis of *DMM* Unit Cell

  (3) 3-D Numerical Modeling of Full-Scale *DMM* Improved Ground

  (4) 2-D Plain Strain Analysis of Full-Scale *DMM* Improved Ground
- **Results and Discussions**
- **Conclusions and Recommendations**

Introduction

(1) The Deep Mixing Method (*DMM*) was developed in Japan as one of soil stabilization methods to improve soft clay for foundation ground in the late of 1970's

(2) In construction, cement slurry is injected into clay layer and in-situ clay is mixed with cement slurry and stabilized by forming strong columns in order to prevent settlement and slip failure

(3) Most of the analysis in Deep Mixing Method (*DMM*) was performed under 2-D plane strain condition

Objective of Study

- To verify the effectiveness of three-dimensional (3-D) finite difference model by *DMM* unit cell analysis.
- To establish a three-dimensional numerical procedure for *DMM* improved ground included two different configurations, namely wall type and pile type under embankment loading.
- To examine the numerical difference of *DMM* improved ground between two dimensional (2-D) plain strain analysis and 3-D analysis.

Literature Review

● The Construction of *DMM* Improved Ground

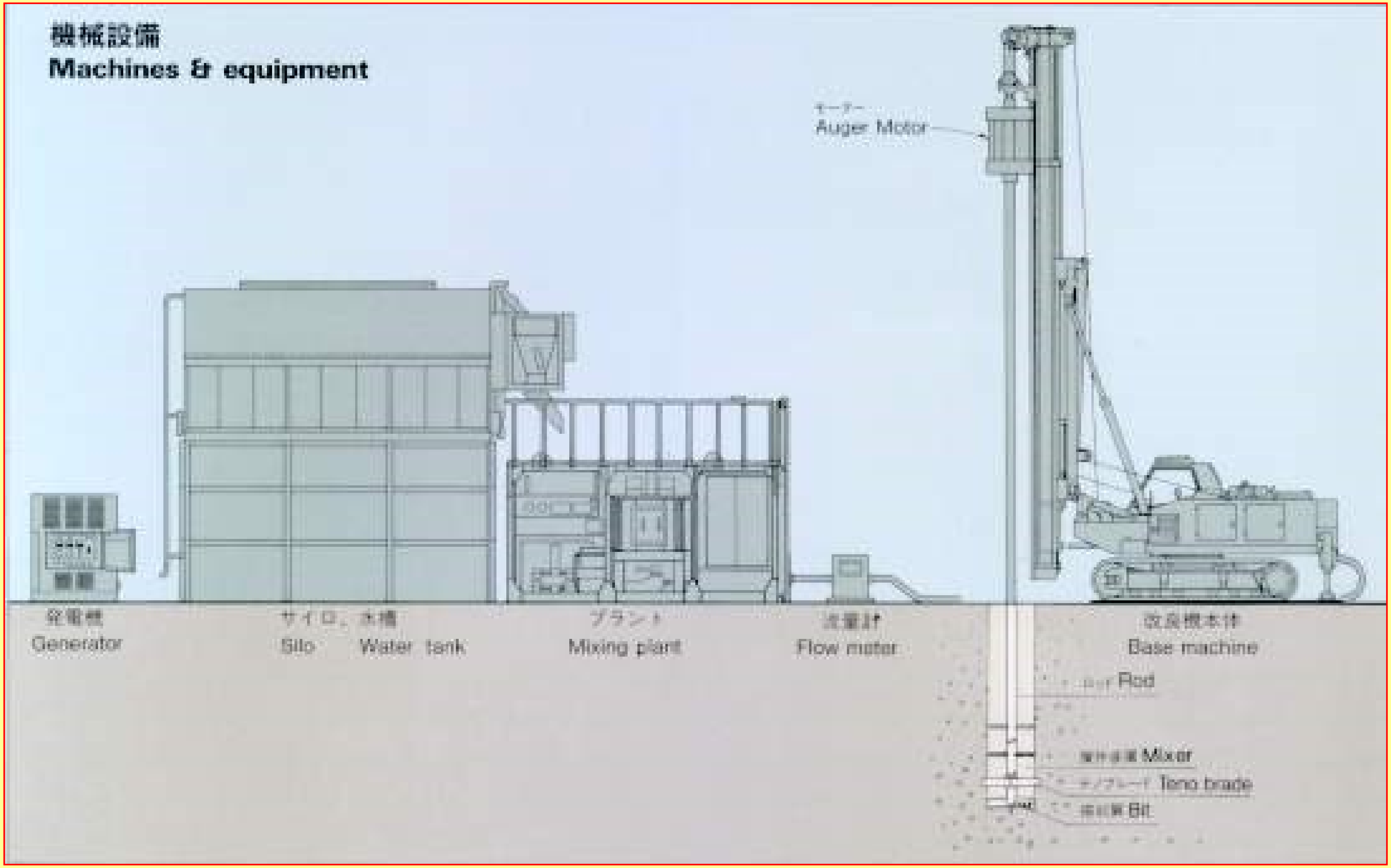

- *DMM* Construction Procedures

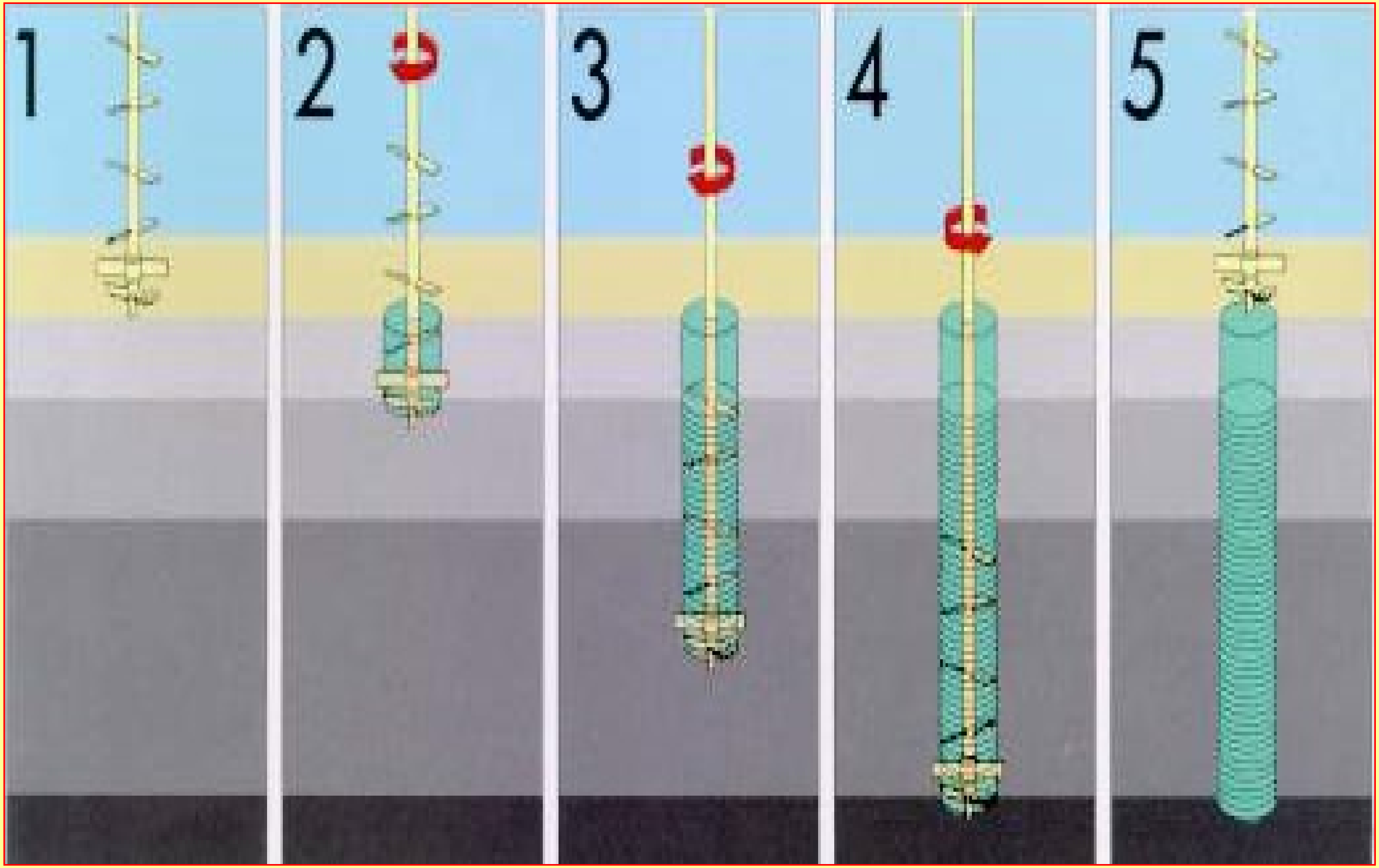

- A most general review of the strength properties of cement stabilization was presented by Mitchell (1976). Mitchell gave the following relationships between q_u and curing time：

$$q_u(t) = q_u(t_o) + K \cdot \log\left(\frac{t}{t_o}\right)$$

$K = 480a_w$ for granular soil and $70a_w$ for fine grain soil

- There are Several Factors Affecting the Strength of the Cement Columns ：
  (1) Type of Cement
  (2) Cement Content
  (3) Curing Time
  (4) Curing Temperature
  (5) Soil Minerals
  (6) Soil pH

Alamgir et al. (1996) proposed that the Mathematic solutions are obtained by using the unit cell concept. The column is considered to be a cylinder, of length *H*, and diameter *dc* *(=2a)*. The unit cell of diameter *de (=2b)*, is loaded with a uniform load *σ0*.

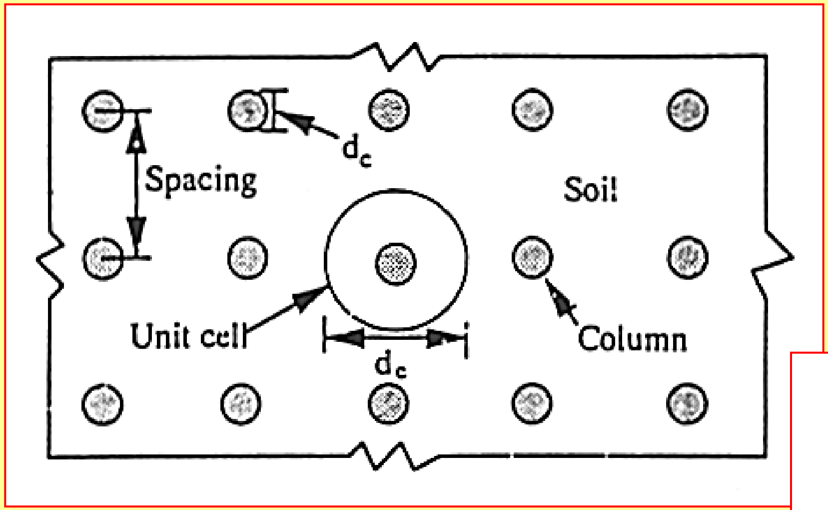

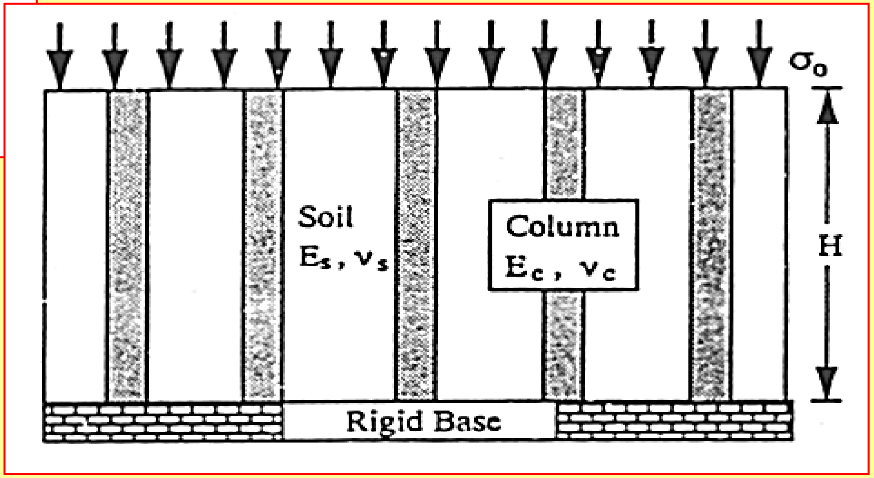

- It is convenient to classify the conventional design methods of *DMM* improved ground ：

(1) The improved ground subjected to vertical loading only

(2) The improved ground subjected to large horizontal loading

(3) The improved ground subjected to small horizontal loading

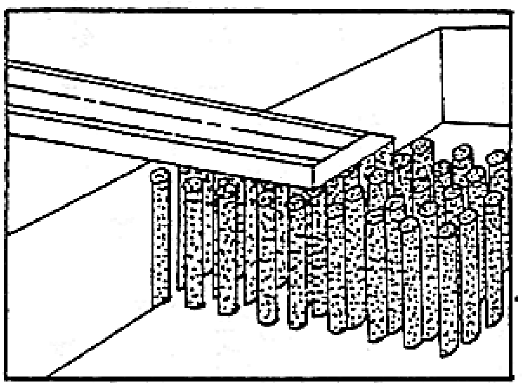

Group column type

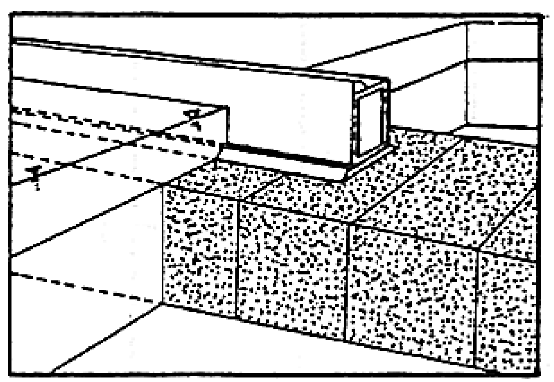

Block type

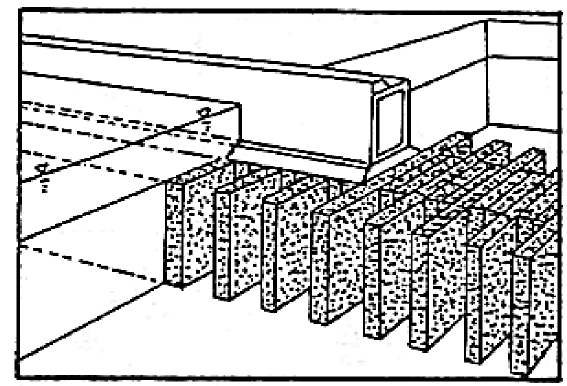

Wall type

Methodology

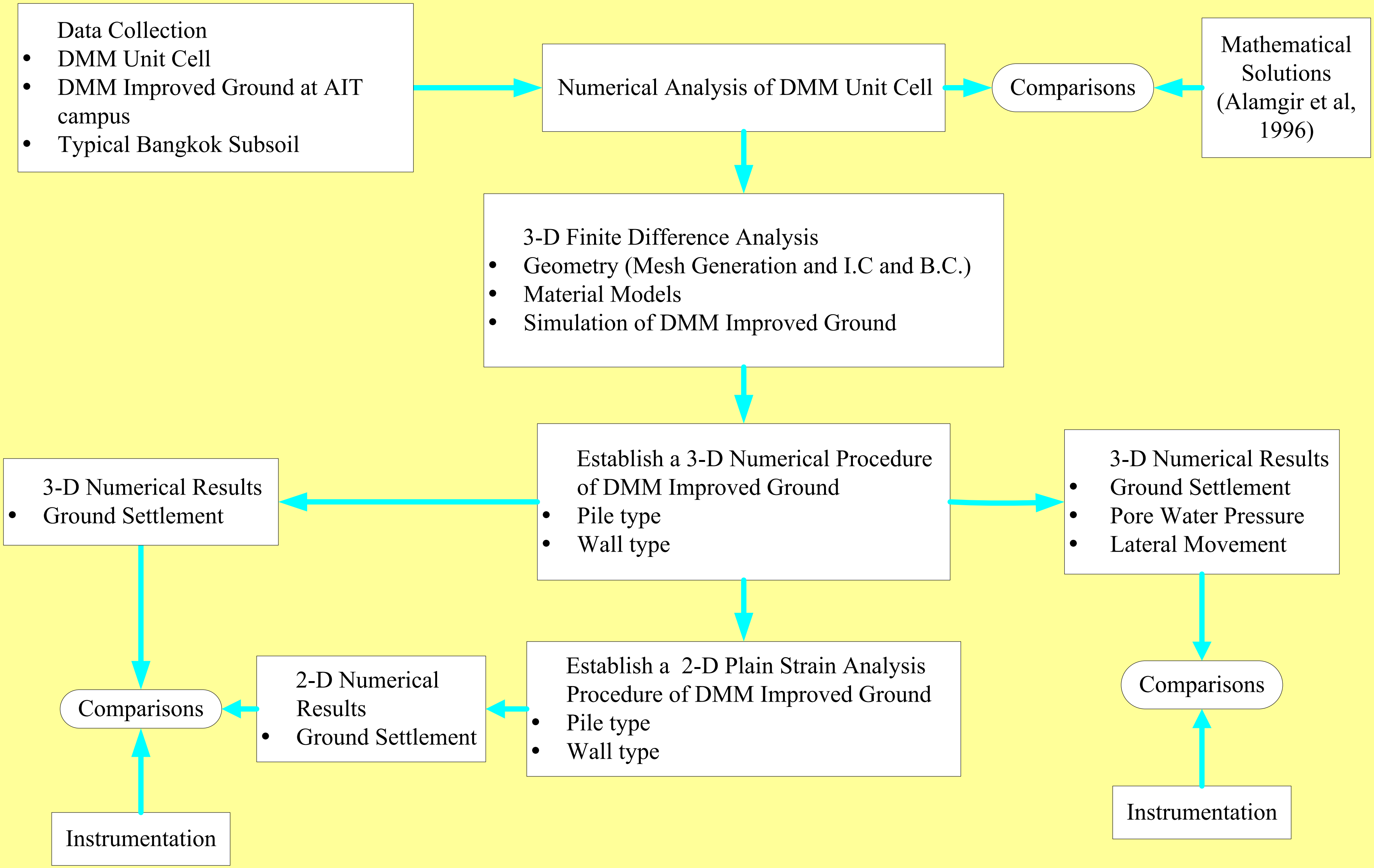

Flowchart of Methodology

Data Collection

Location of Borehole and In-situ Test

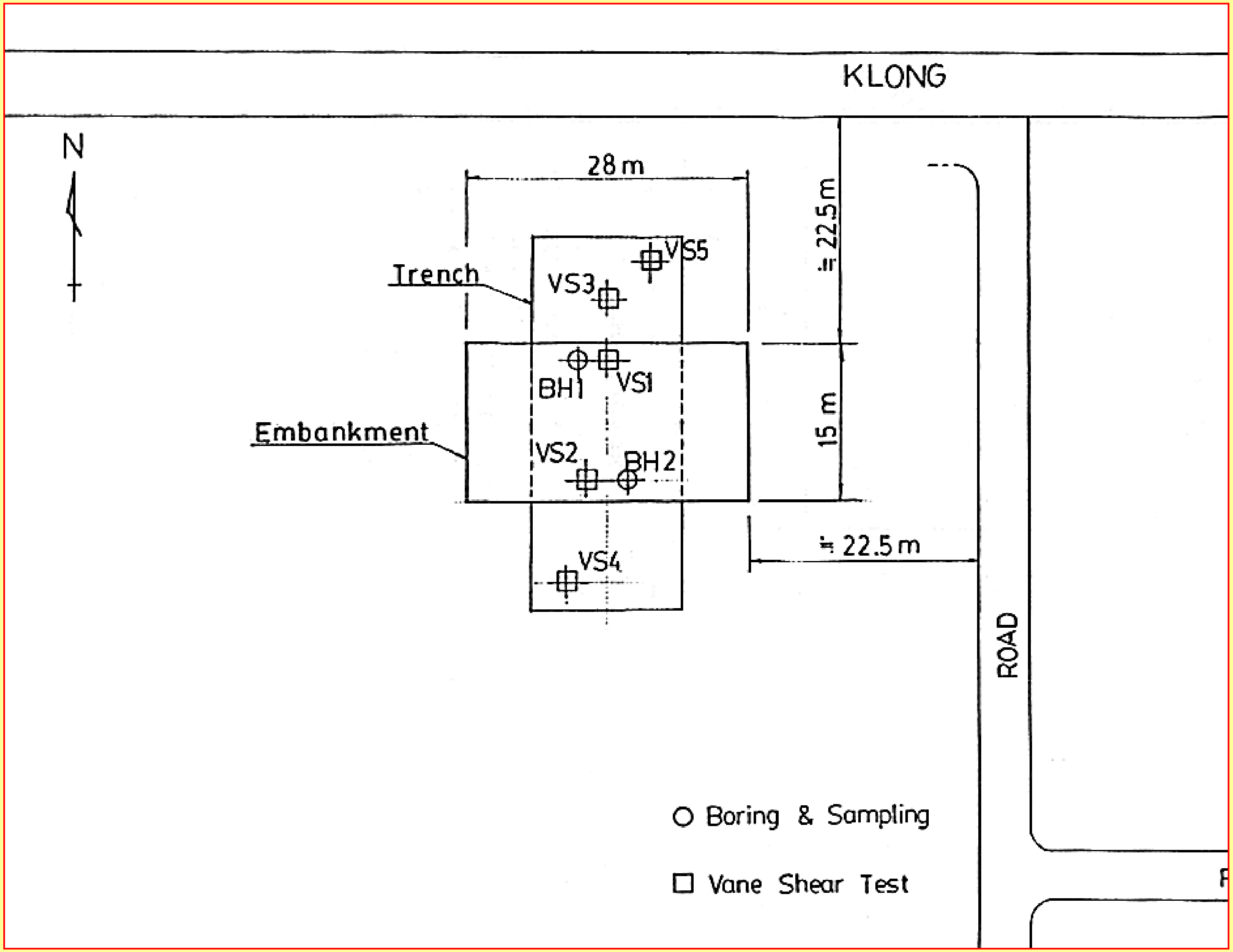

Soil Boring Log

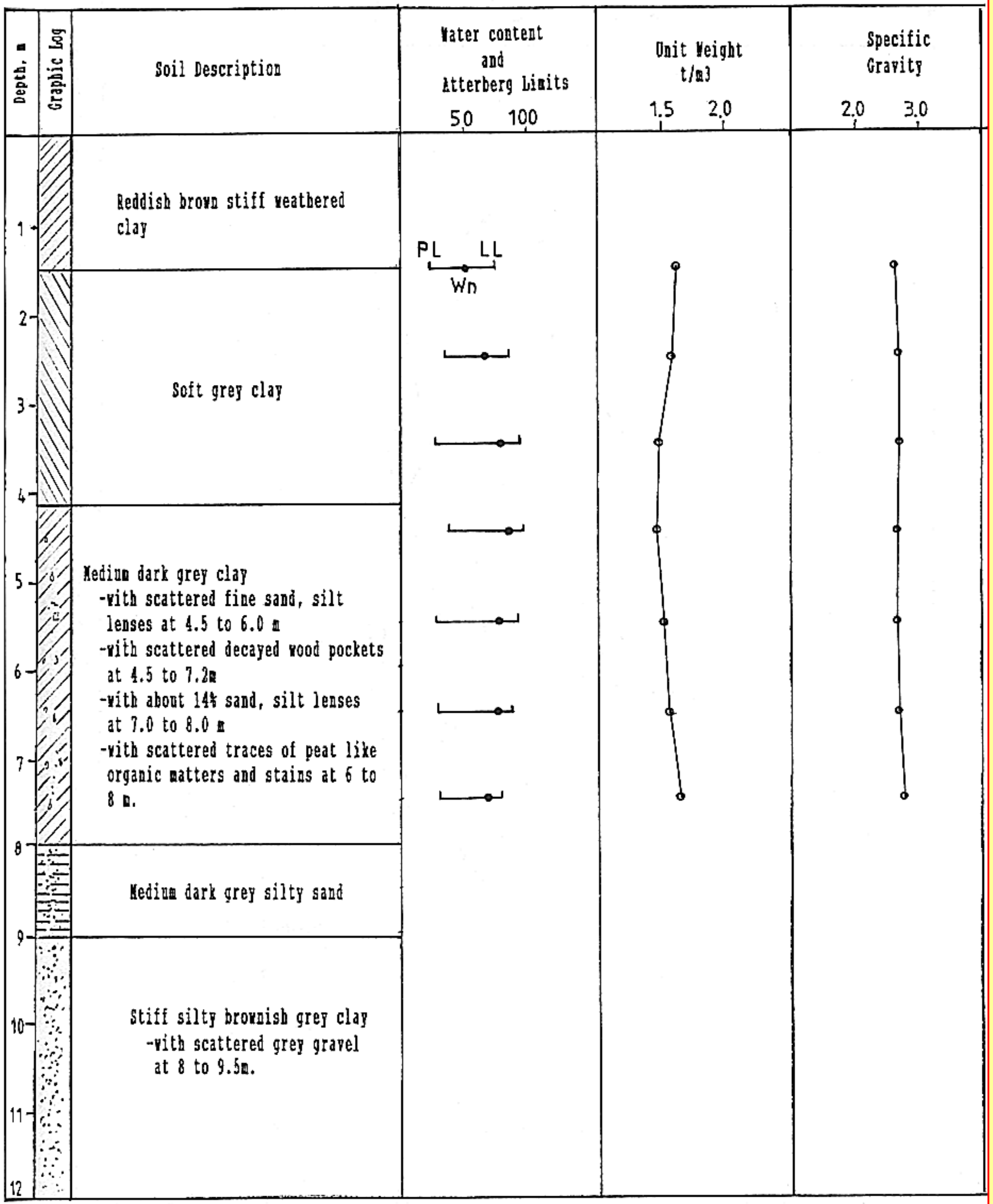

Undrained Shear Strength of Various Tests

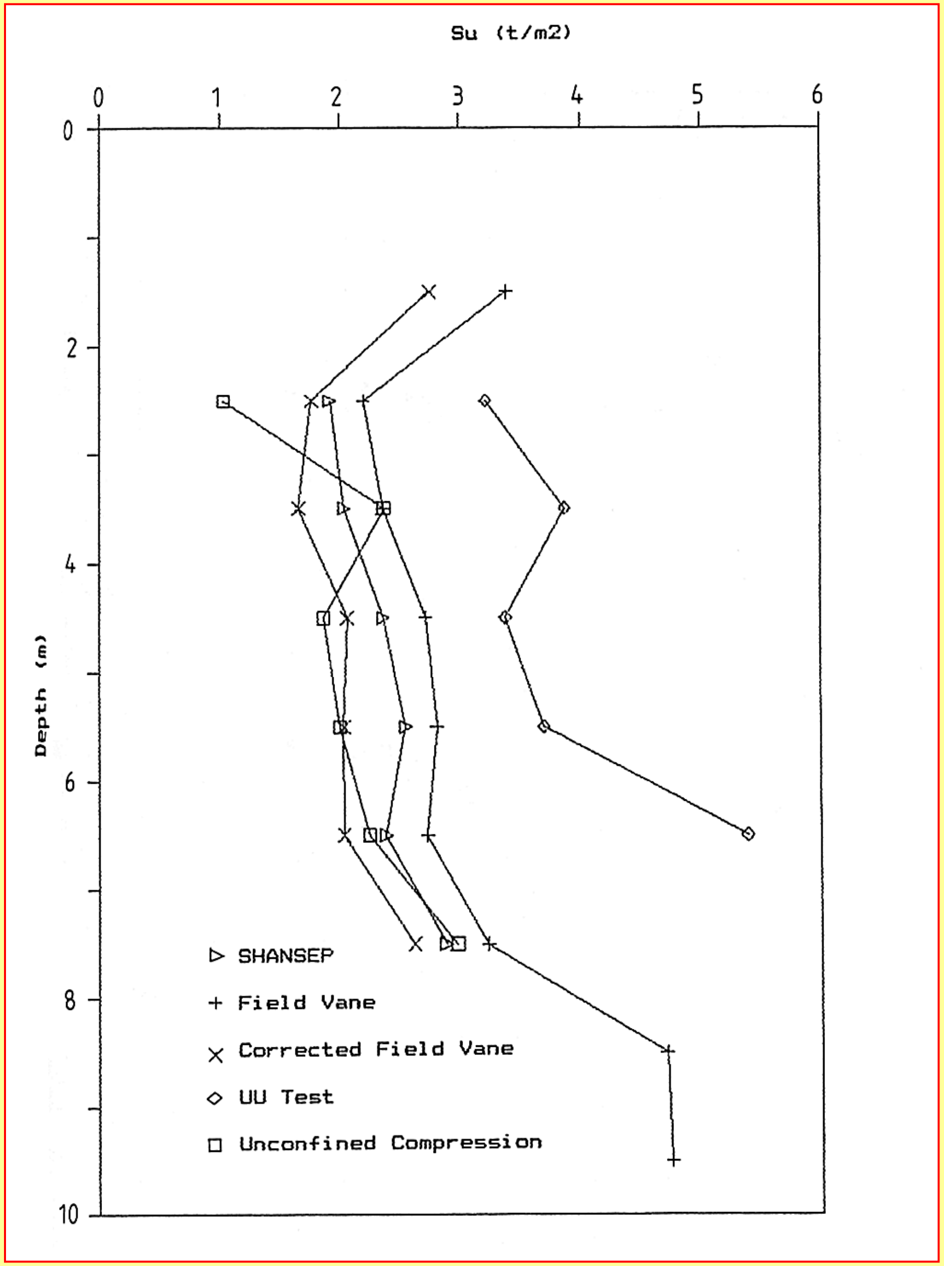

SHANSEP

Field Vane Test

Corrected Field Vane Test

UU Test

Unconfined Compression

Consolidation Tests of Soil Samples from Filed Site

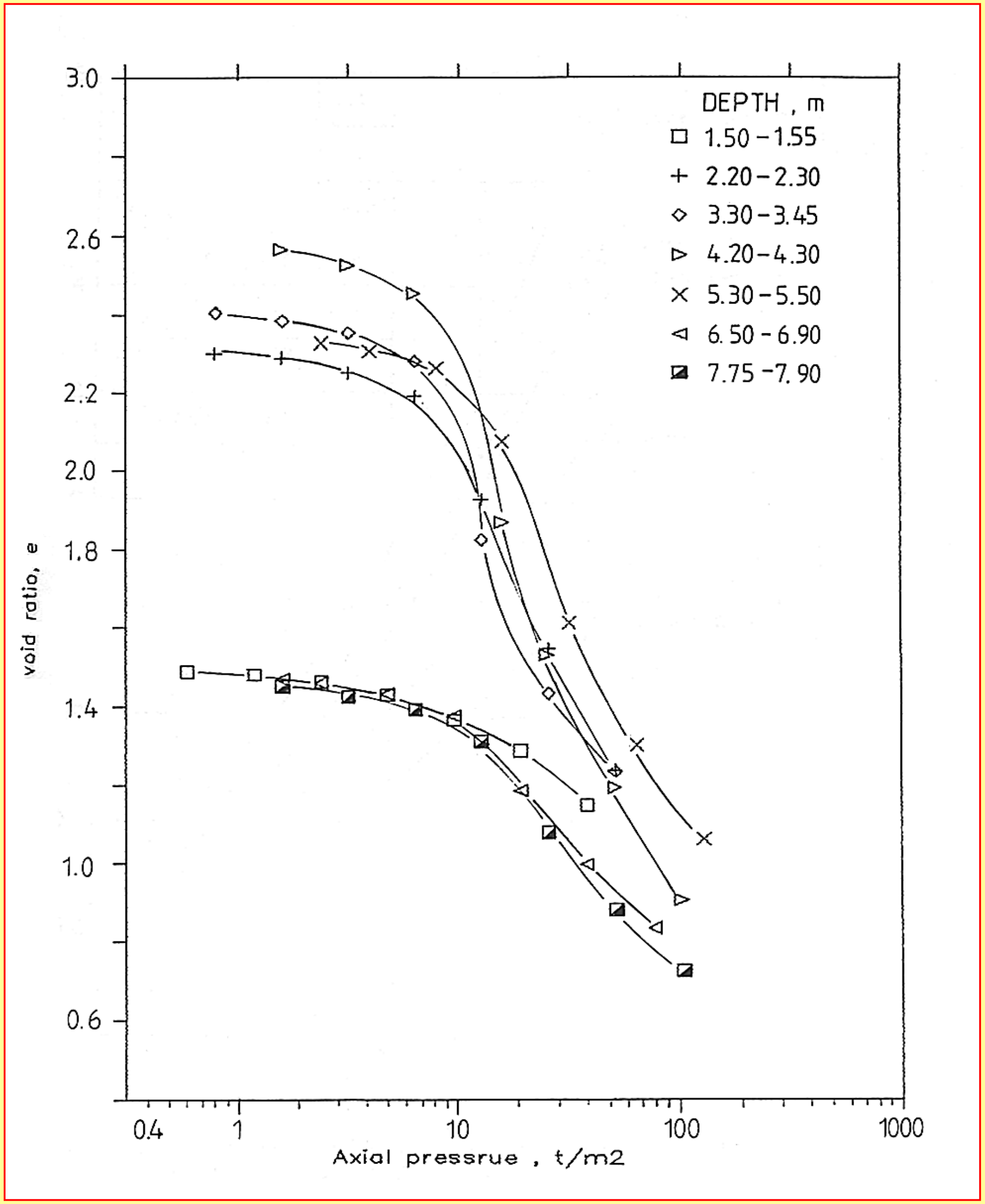

qu-aw of Laboratory-Mixed Sample

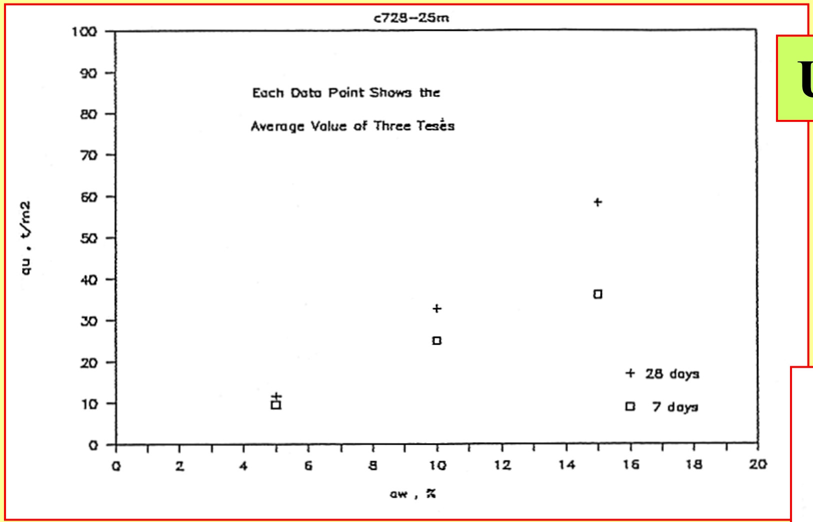

Untreated Soil from Depth of 2.5*m*

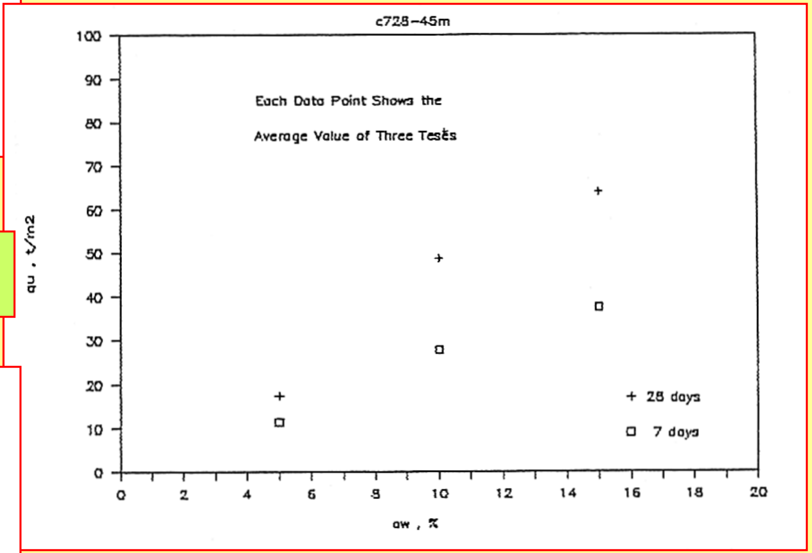

Untreated Soil from Depth of 4.5*m*

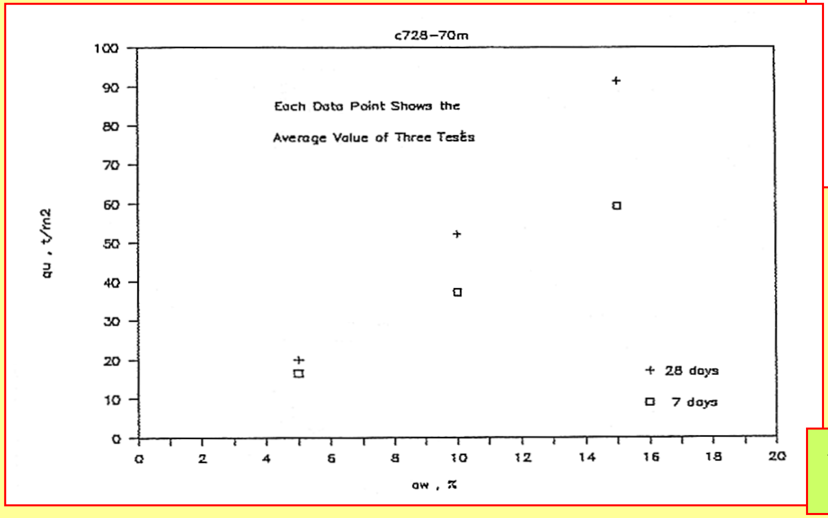

Untreated Soil from Depth of 7.0*m*

Numerical Analysis of *DMM* Unit Cell

Finite Difference Mesh of Cement Treated Unit Cell

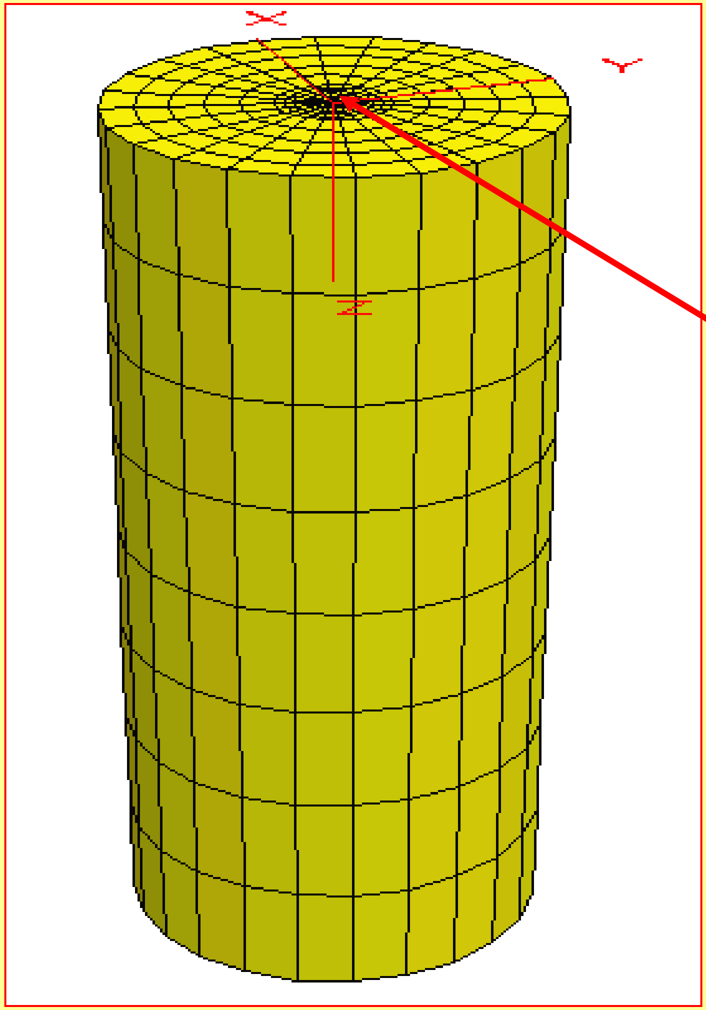

cement column

Geometry Model of Cement Treated Unit Cell

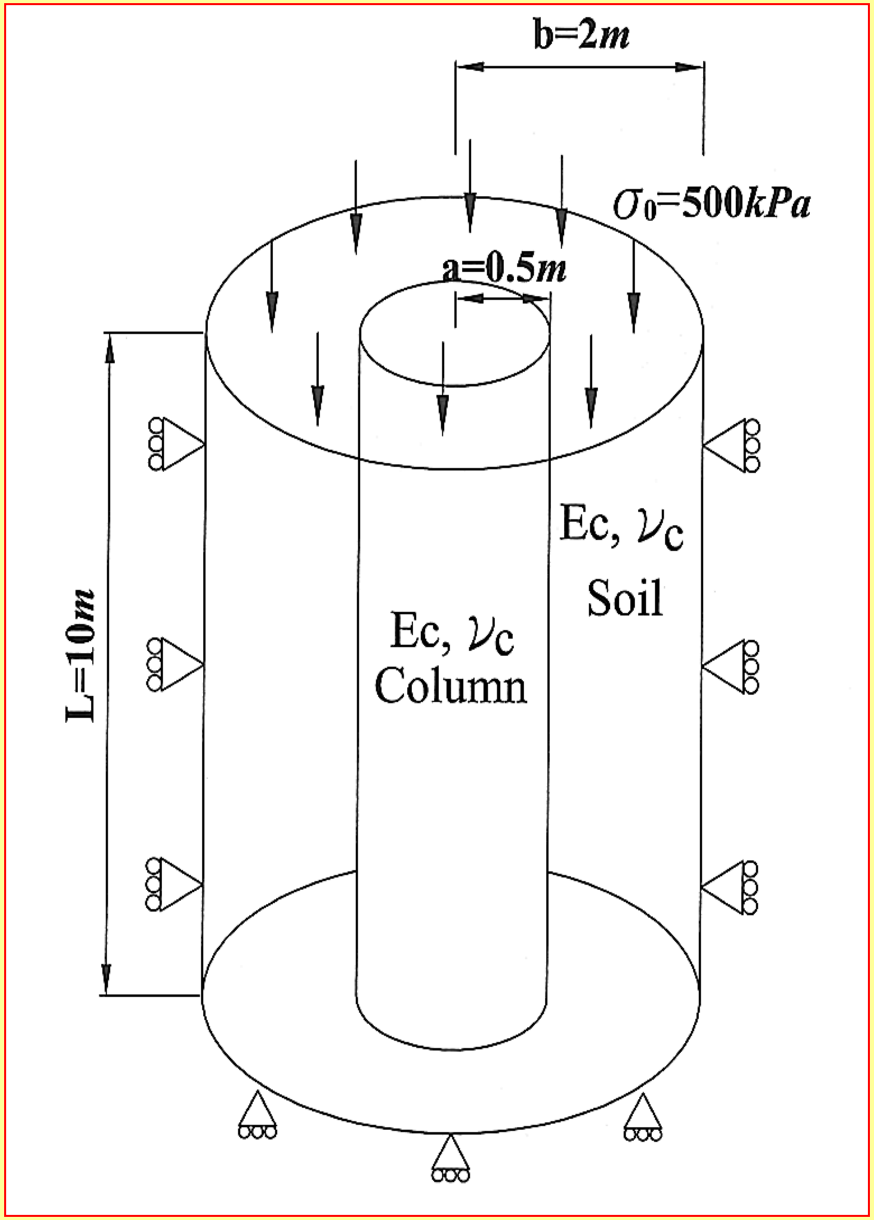

Input Parameters for Numerical Analysis of Cement Treated Unit Cell

	Model	Apply load σ_0 (kPa)	E (x10^3kpa)	K (x10^3kpa)	G (x10^3kpa)	v	γ (kN/m^3)
Soil	Linear-elastic	500	5	8.33	1.79	0.4	13.73
Column	Linear-elastic	500	50	27.78	20.83	0.2	13.73

$L/a = 20$, n $(= b/a) = 4$, $\sigma_o/E_s = 0.10$, $E_c/E_s = 10$, $a = 0.5$ m

Comparison of Settlement Profile of Cement Treated Unit Cell

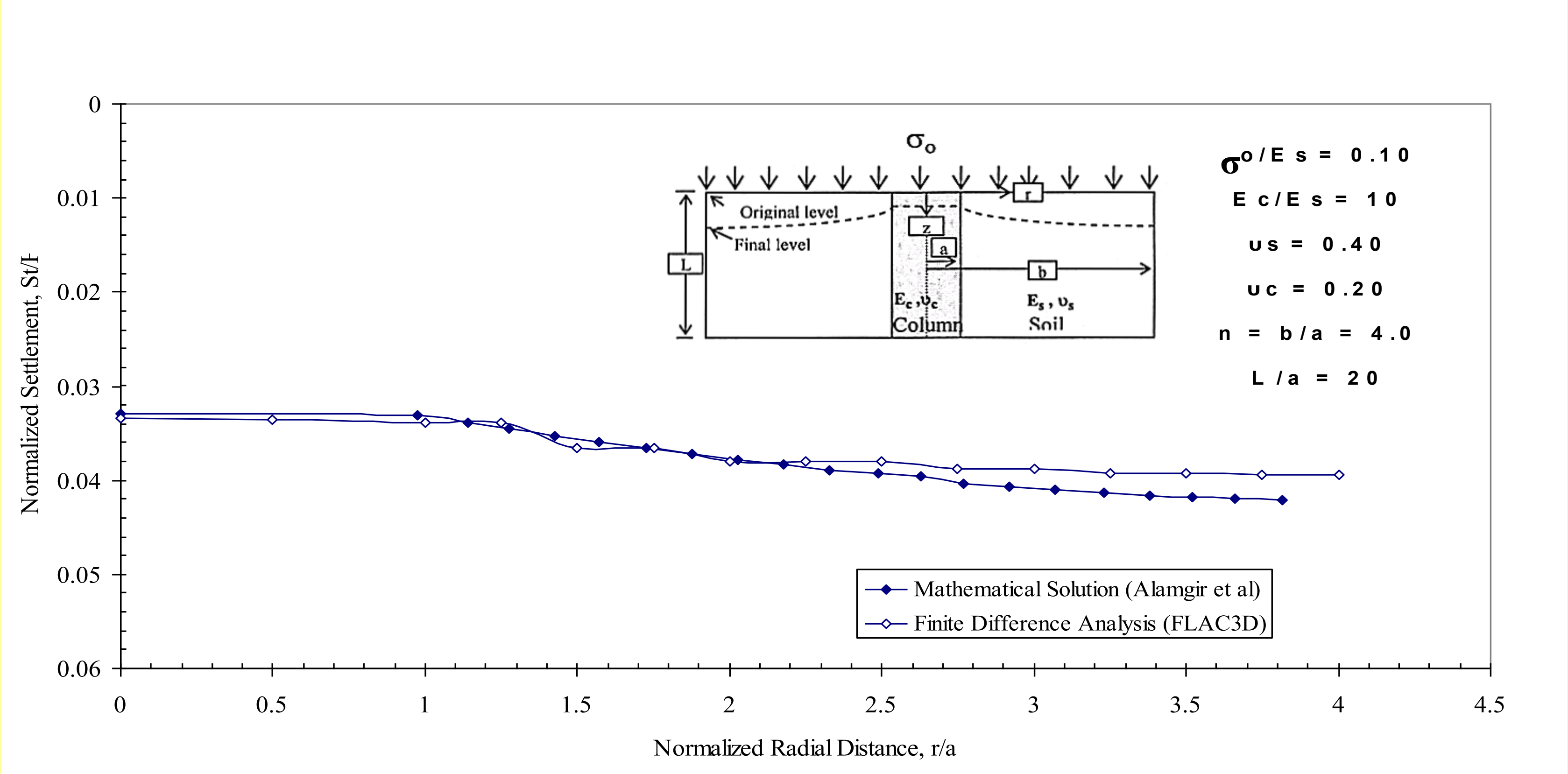

Stress Concentration Ratio with Depth of Cement Treated Unit Cell

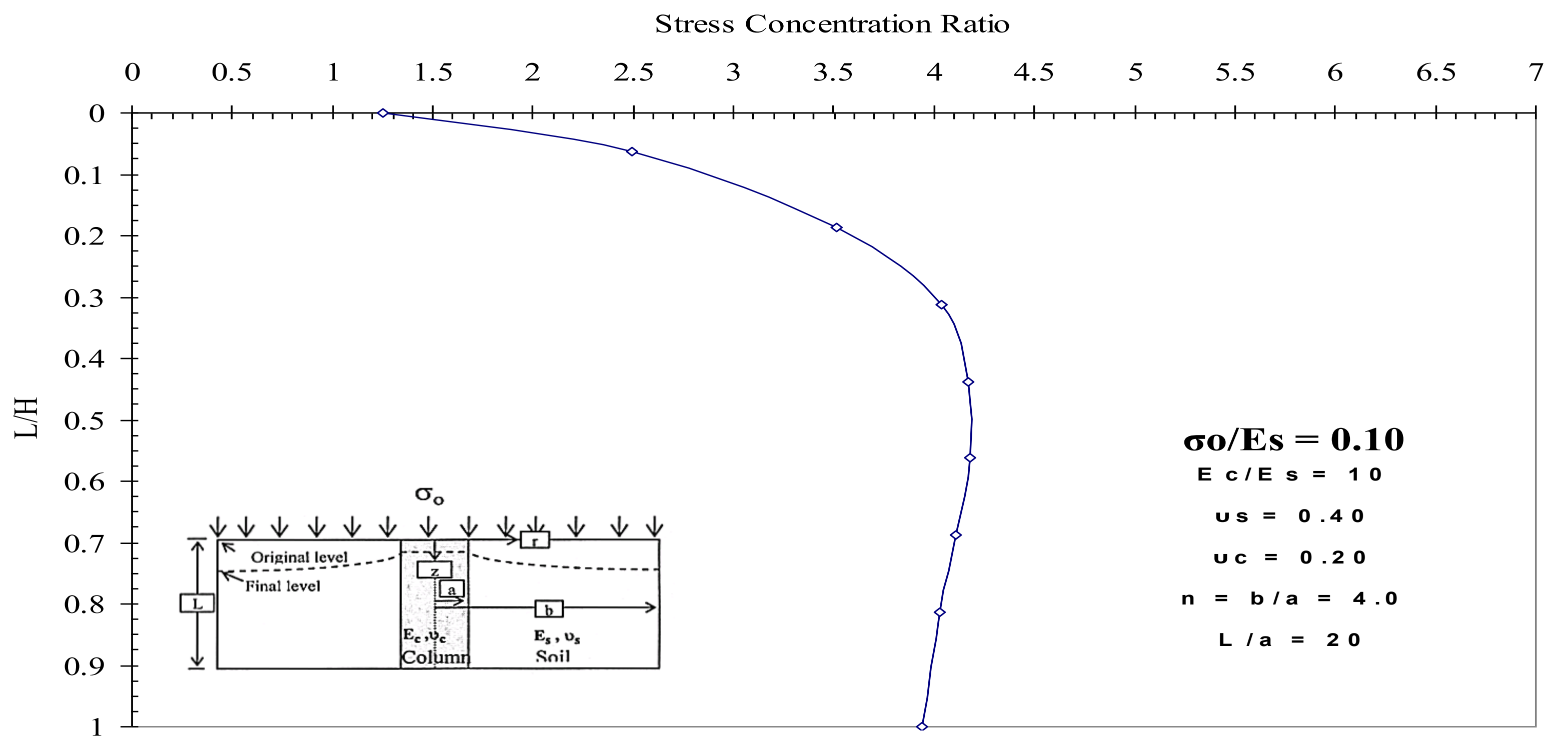

3-D Numerical Modeling of Full-Scale *DMM* Improved Ground

Construction of Testing Embankment on *DMM* Improved Ground

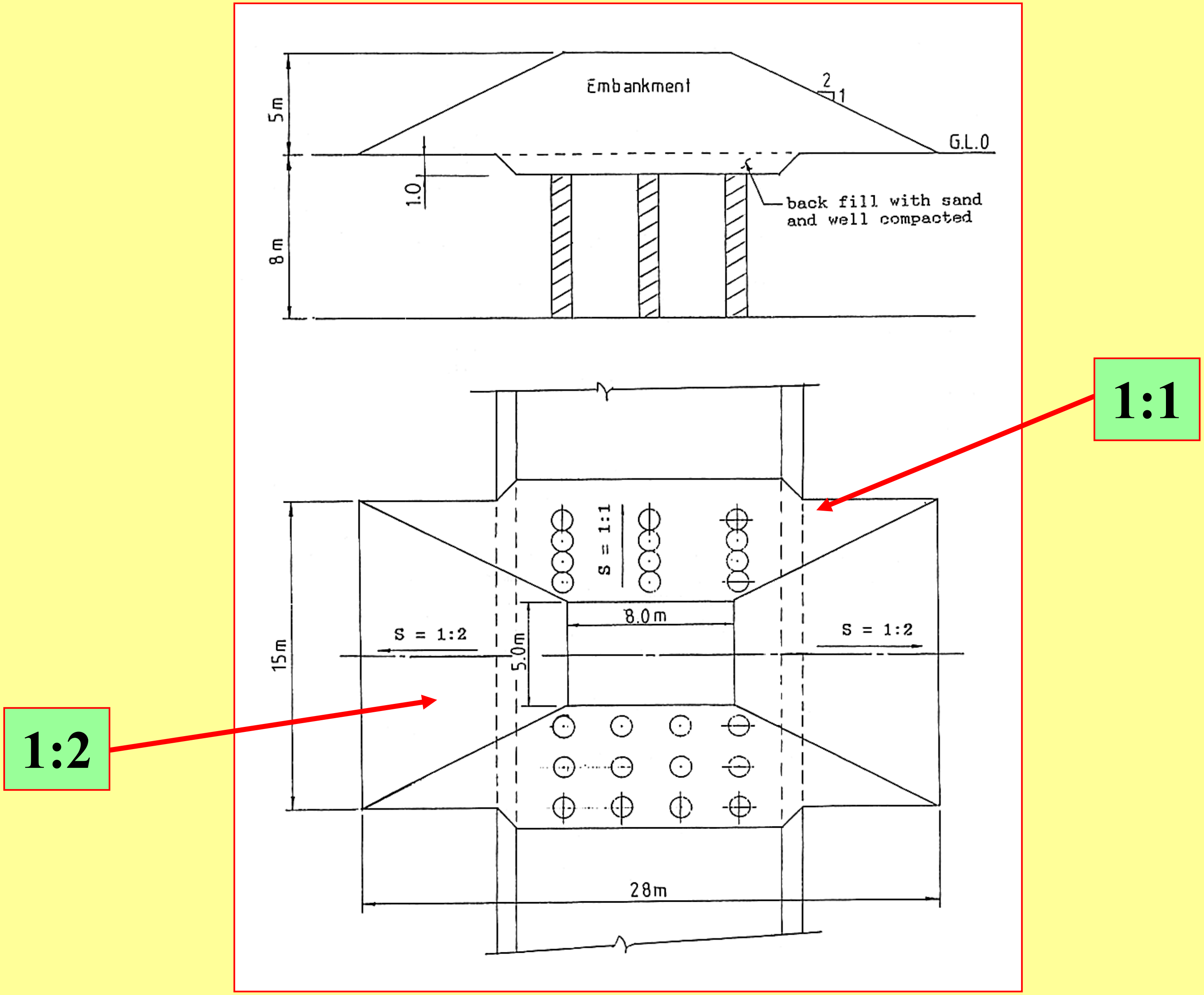

Finite Difference Mesh of Testing Embankment on *DMM* Improved Ground

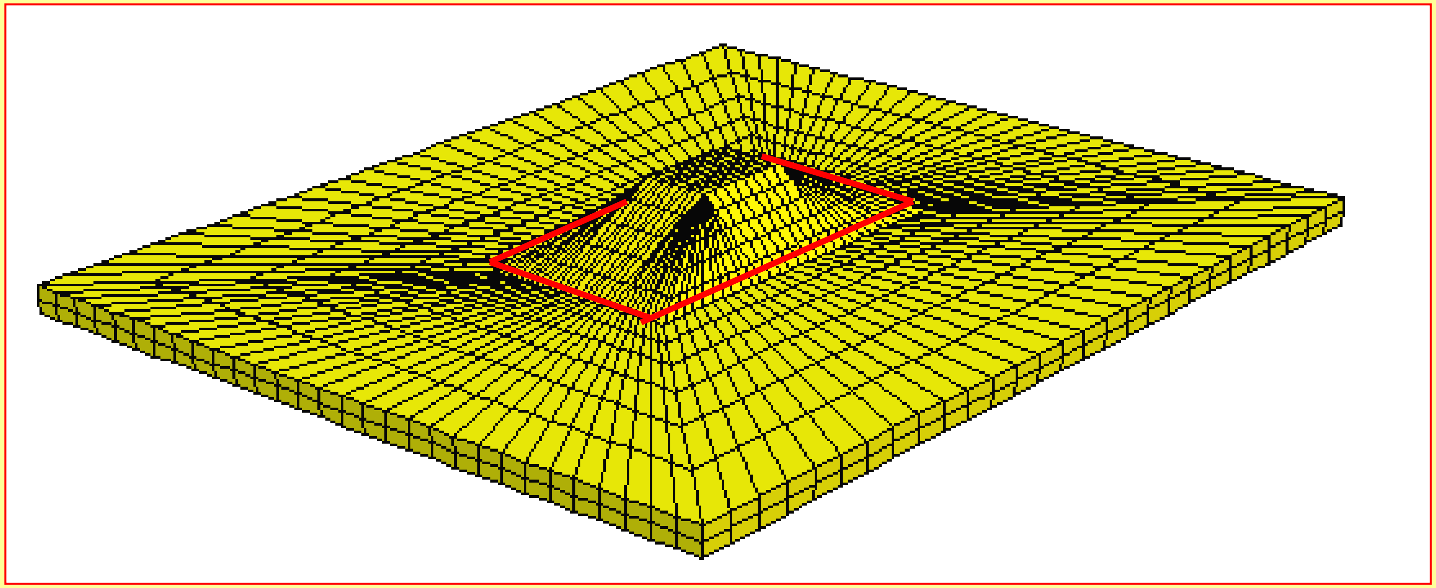

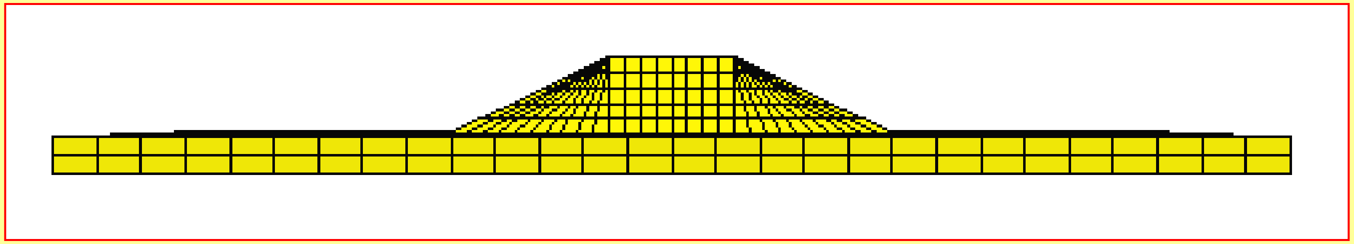

Equivalent Surcharge Pressures due to Stage Construction of Testing Embankment

Number of Lift (m)	Equivalent incremental Surcharge $\Delta\sigma_z$ (kPa)	Equivalent Cumulative Surcharge σ_z (kPa)
1	13.87	13.87
2	15.51	29.38
3	14.73	44.11
4	13.8	57.91
5	11.24	69.15

Surcharge Pressure on *DMM* Improved Ground Due to Construction of Testing Embankment

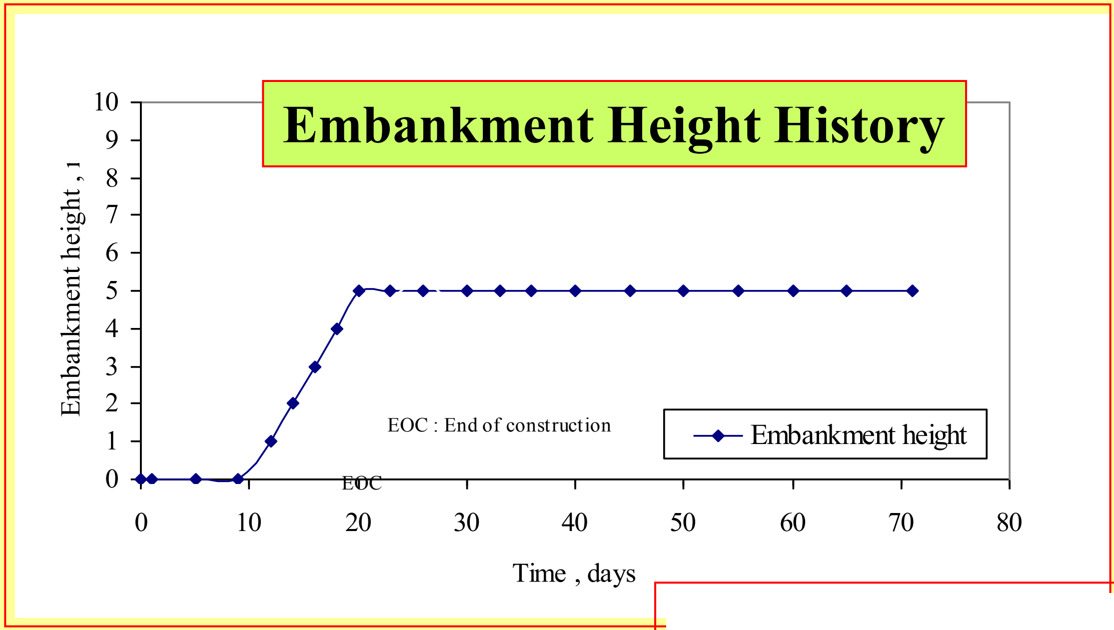

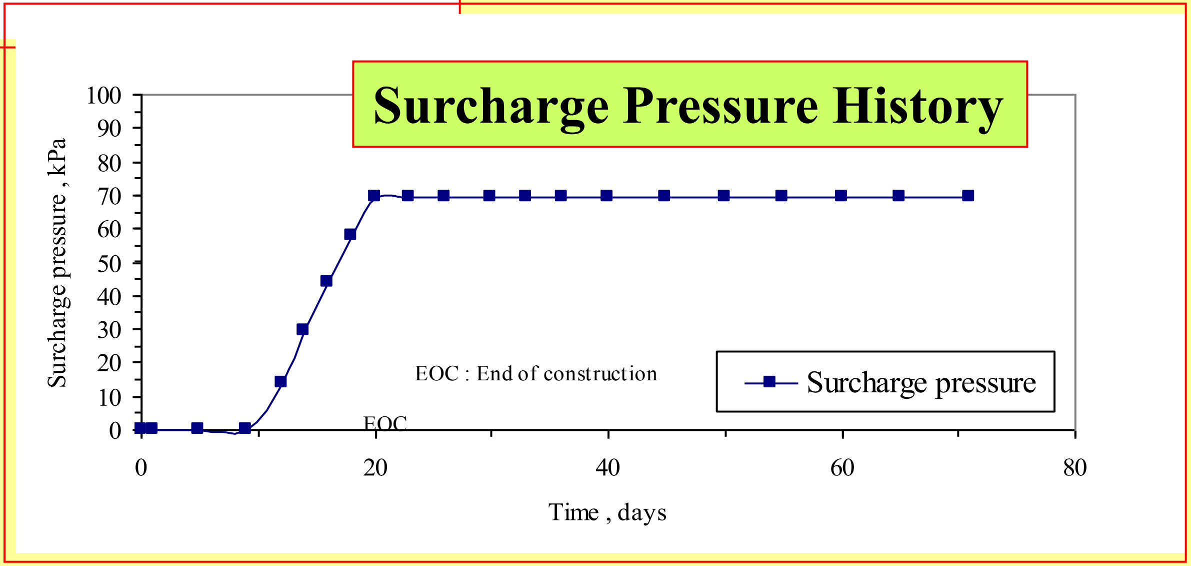

Finite Difference Mesh of Full Scale *DMM* Improved Ground for 3-D Numerical Analysis

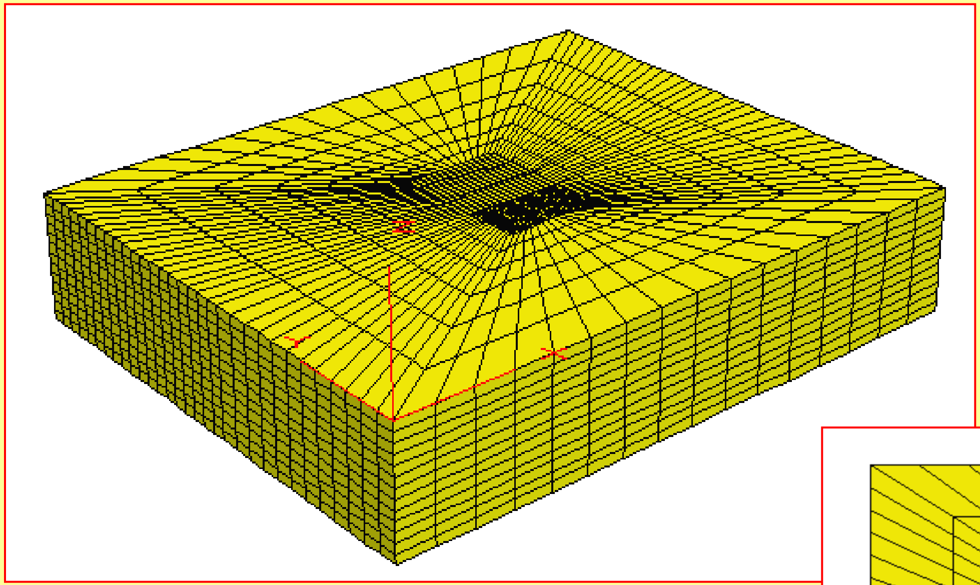

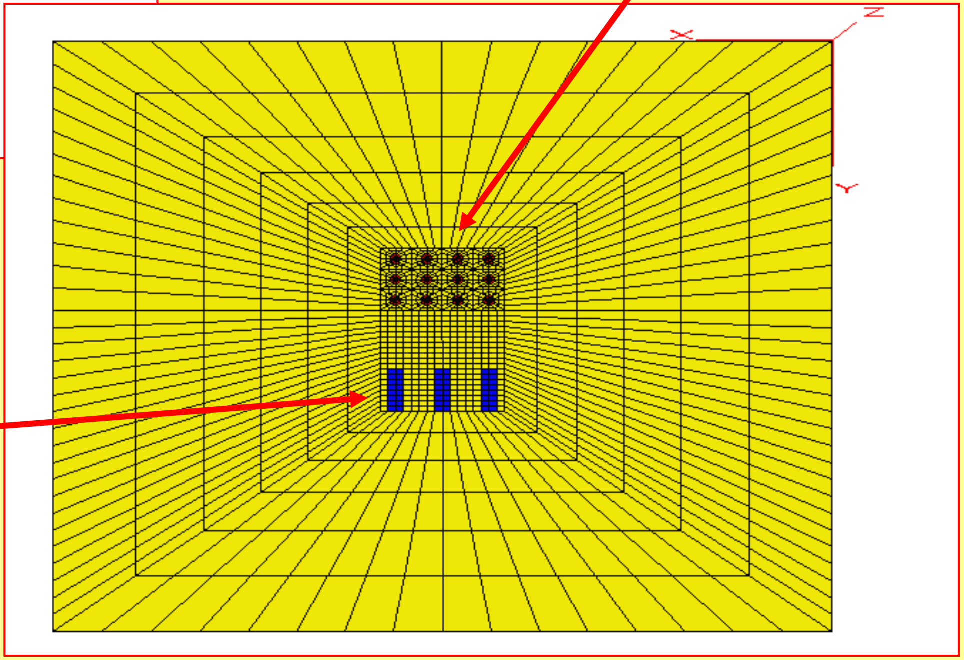

Pile Type Improvement

Wall Type Improvement

Geometry of Full-Scale *DMM* Improved Ground at *AIT* Campus

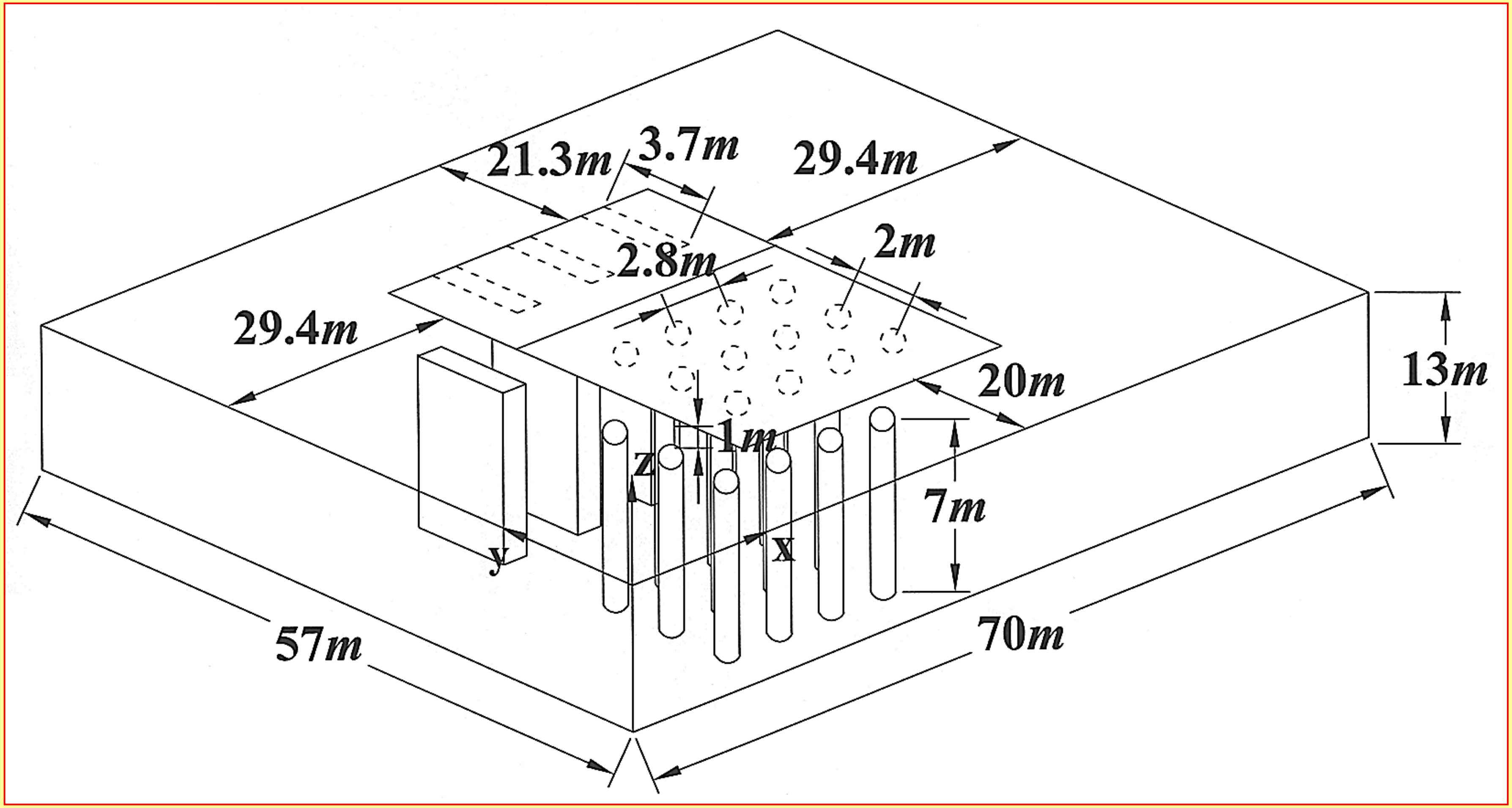

Layout of Various Instrumentations

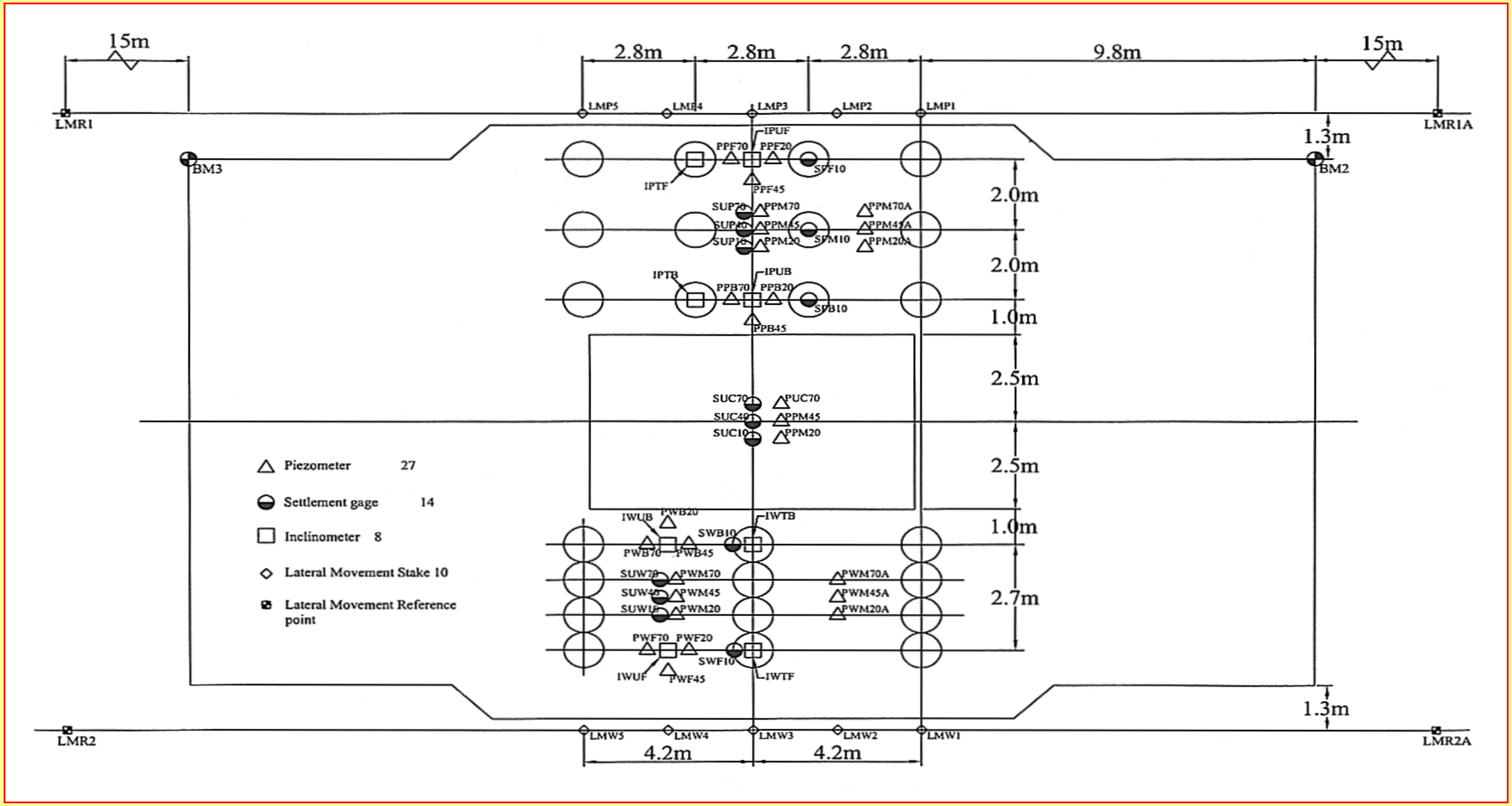

Selected Instrumentations for Numerical Comparison

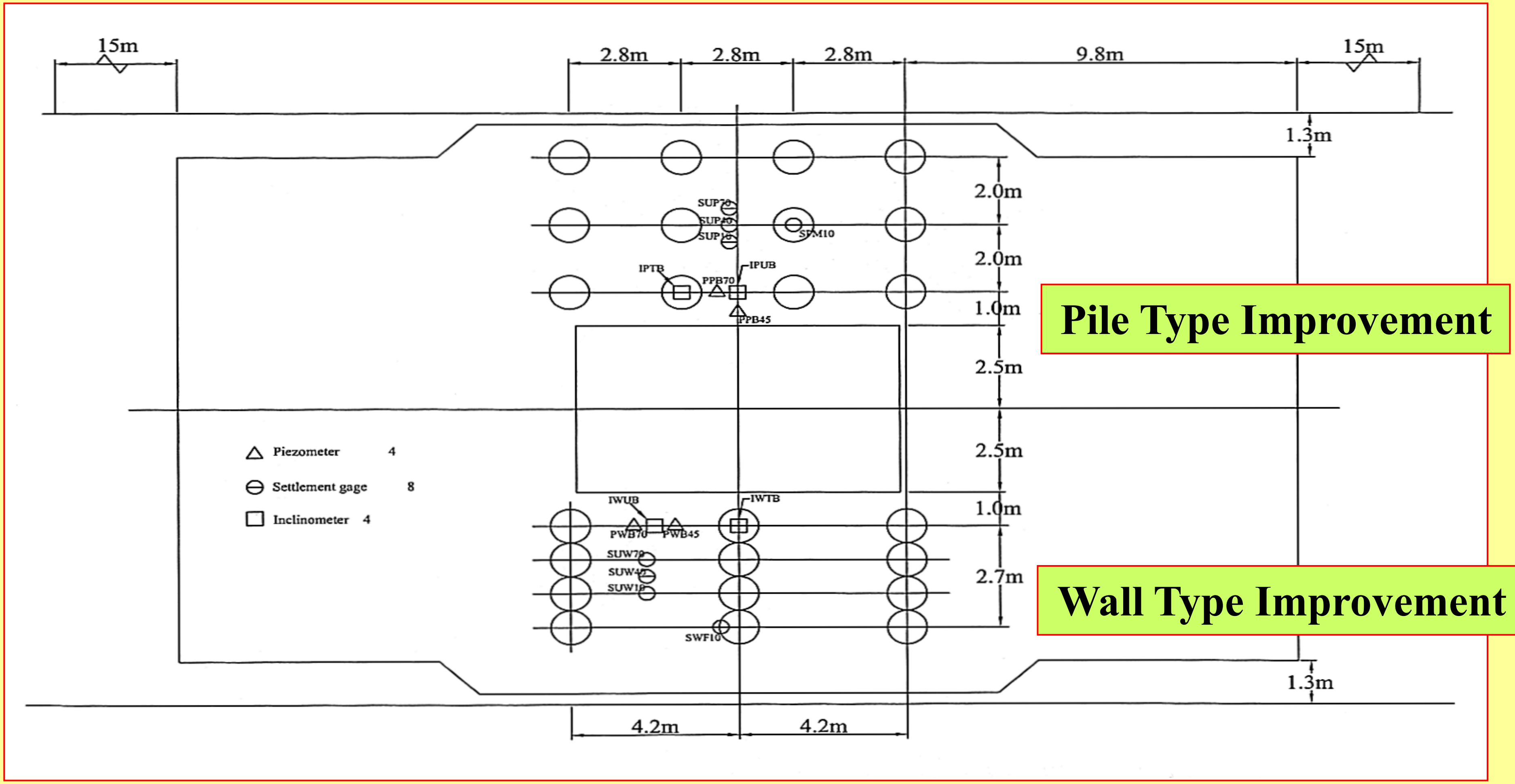

Settlement

Pore Pressure

Lateral Movement

Unconfined Compressive Tests of In-situ Mixed Sample

Sample No.	Depth m	Cement content α kg/m^3	a_w %	q_u t/m^2		E_{50} t/m^2		Remark
CSB1-70A	7.0	150	15	31.45		3990		Wall type
CSB2-25A	2.5	100	10	17.07	Avg.	1547	Avg.	Pile type
CSB2-25	2.5	100	10	23.22	22.74	1596	2872	Pile type
CSB2-50	5.0	100	10	27.94		5488		Pile type

Failure Criterion of Modified Cam-Clay Model (*FLAC*3D)

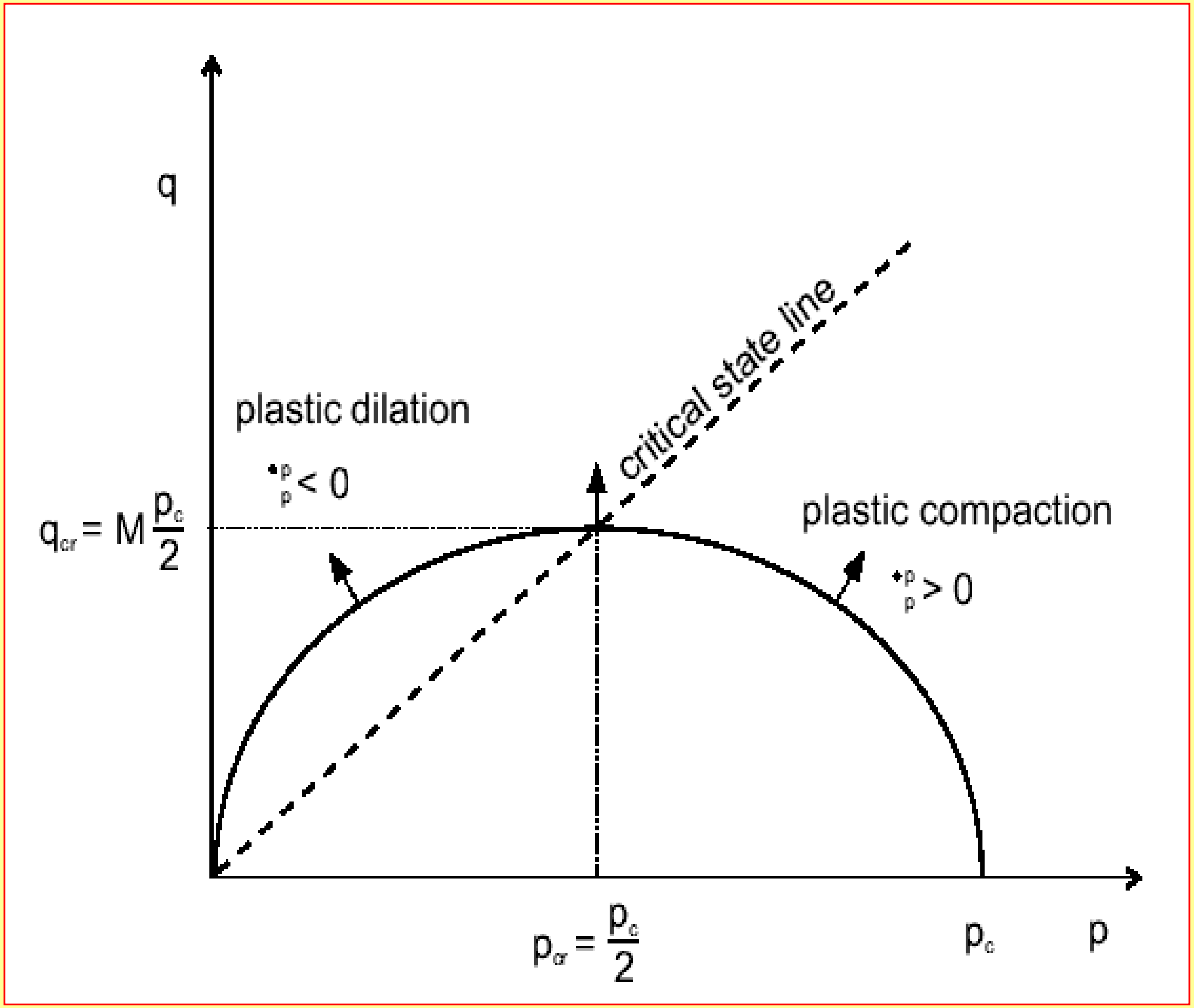

Normal Consolidation Line and Swelling Line for an Isotropic Compression Test for Modified Cam-Clay Model (*FLAC*3D)

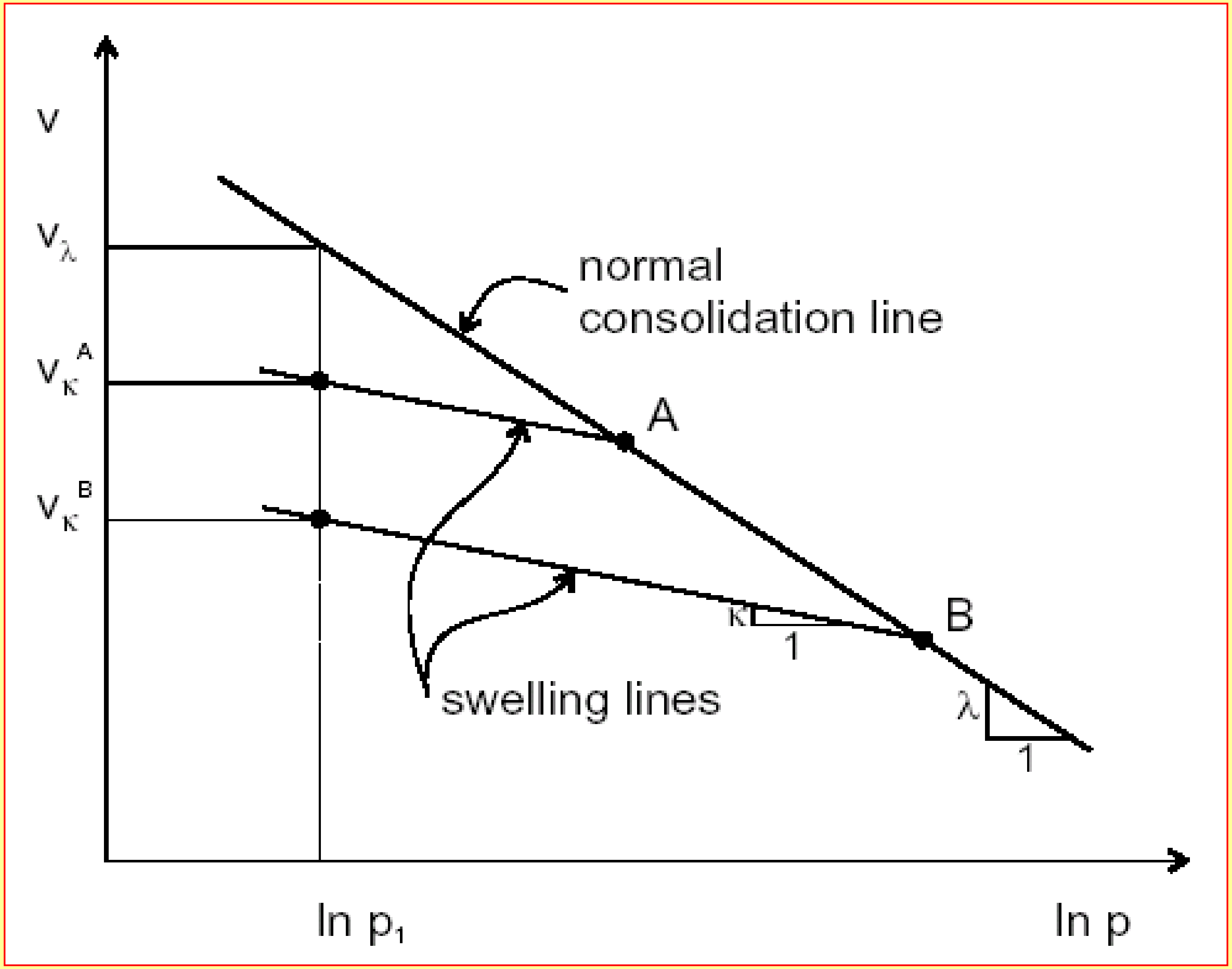

Input Parameters for 3-D Finite Difference Analysis of *DMM* Improved Ground

Depth (m)	K (x10^3kpa)	G (x10^3kpa)	M	λ	k	p_{c0} (x10^3kpa)	p_1 (Pa)	υ_λ	k (cm/sec)	n
2.0-4.0	1.46	0.56	0.899	0.481	0.0962	0.109	1	8.792	1.23×10^{-7}	0.701
4.0-6.0	1.67	0.64	0.899	0.486	0.0972	0.123	1	9.022	1.62×10^{-7}	0.71
6.0-8.0	2.30	0.88	0.899	0.251	0.0502	0.125	1	5.352	9.80×10^{-8}	0.593

Input Parameters for Modified Cam-clay Model

Mohr-Coulomb Failure Criterions (*FLAC*3D)

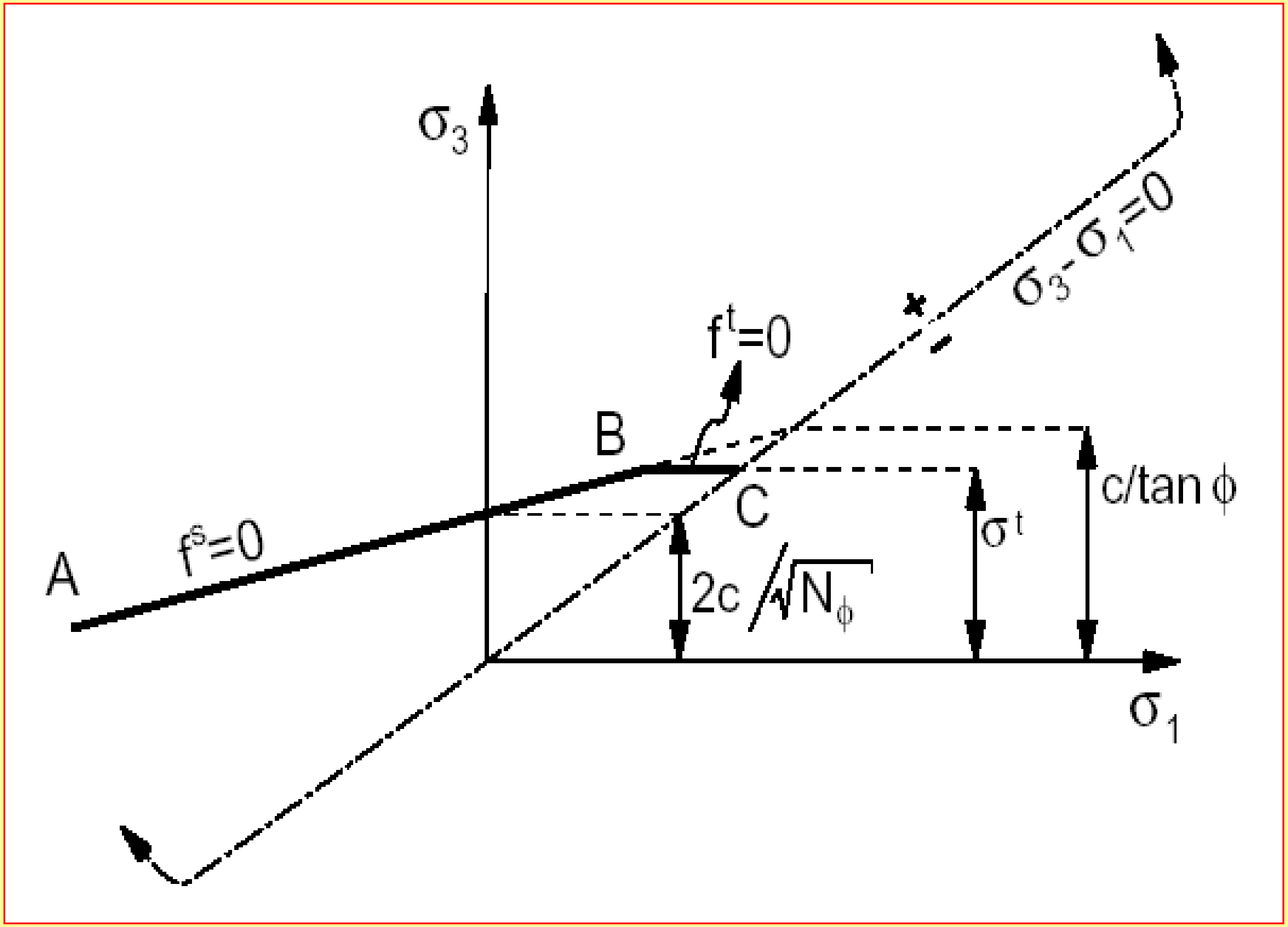

Input Parameters for Mohr-Coulomb Model

Depth (m)	K (x10^3 kpa)	G (x10^3 kpa)	c' (kPa)	ϕ' ($deg.$)	σ^t (kPa)	ψ ($deg.$)	k (cm/sec)	n
0.0-2.0	2	1.2	30	28	56.42	0	2.20×10^{-7}	0.597
8.0-9.0	12.2	4.68	10	30	17.32	0	1.50×10^{-6}	0.35
9.0-13.0	4.67	2.8	15	28	28.21	0	1.62×10^{-7}	0.615
Backfill	2	1.2	30	28	56.42	0		
Pile Type	18.78	11.27	20	36	27.53	0	2.50×10^{-8}	0.399
Wall Type	26.09	15.66	20	36	27.53	0	2.50×10^{-8}	0.399

$\sigma^t = c'/\tan\phi'$ = tension limits

Comparison of Settlement between 3-D Numerical Prediction and Field Observation for Treated and Untreated Zones

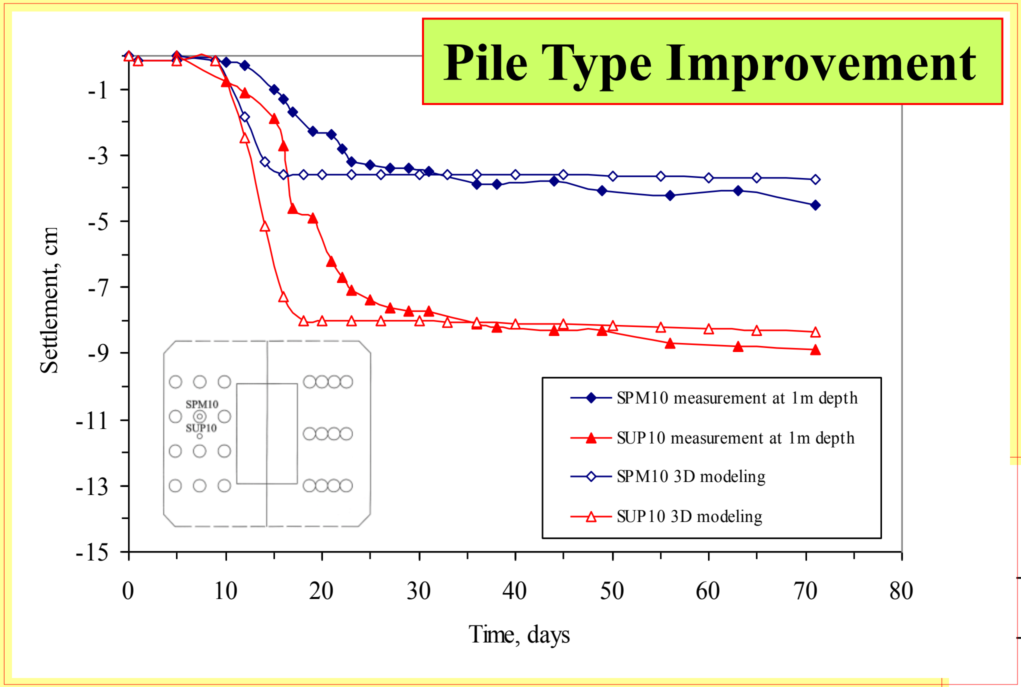

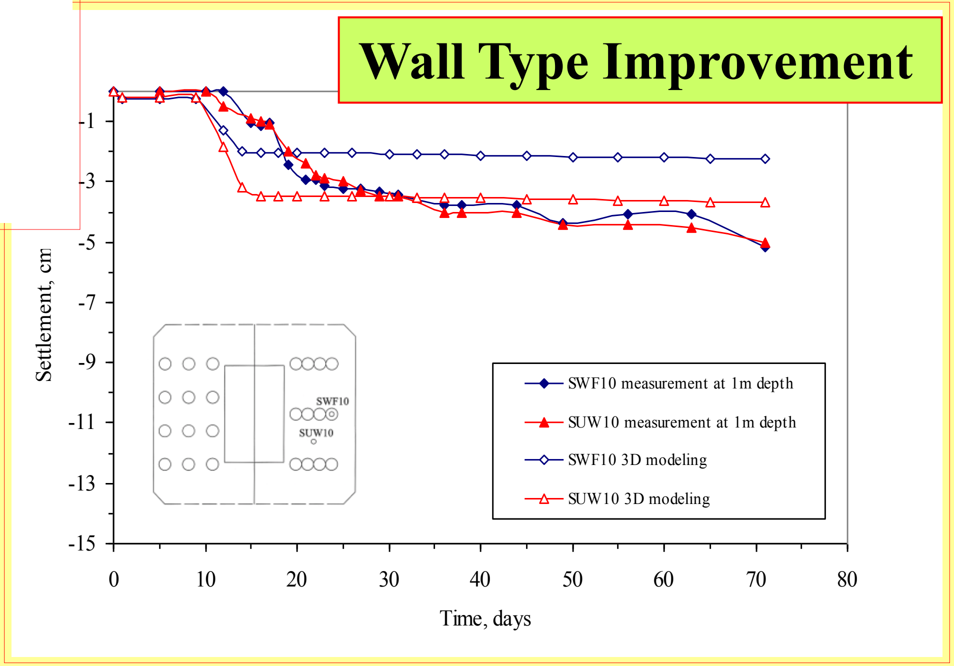

Comparison of Settlement between 3-D Numerical Prediction and Field Observation for Untreated Zone

Pile Type Improvement

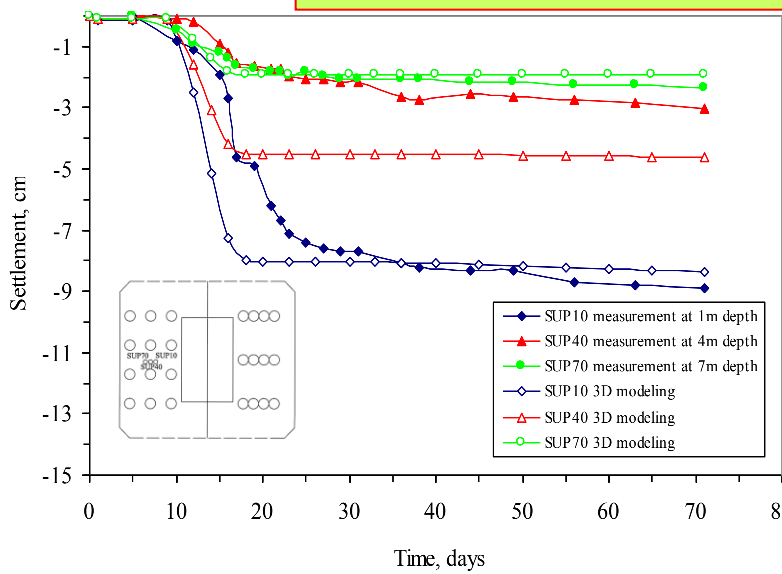

Wall Type Improvement

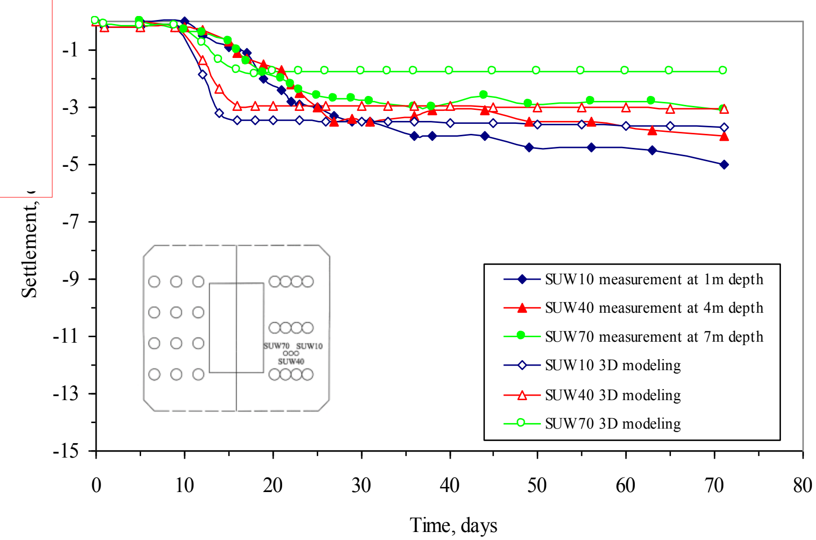

Z-Displacement (Settlement) Contours of the *DMM* Improved Ground of Pile Type at the End of Instrumentation

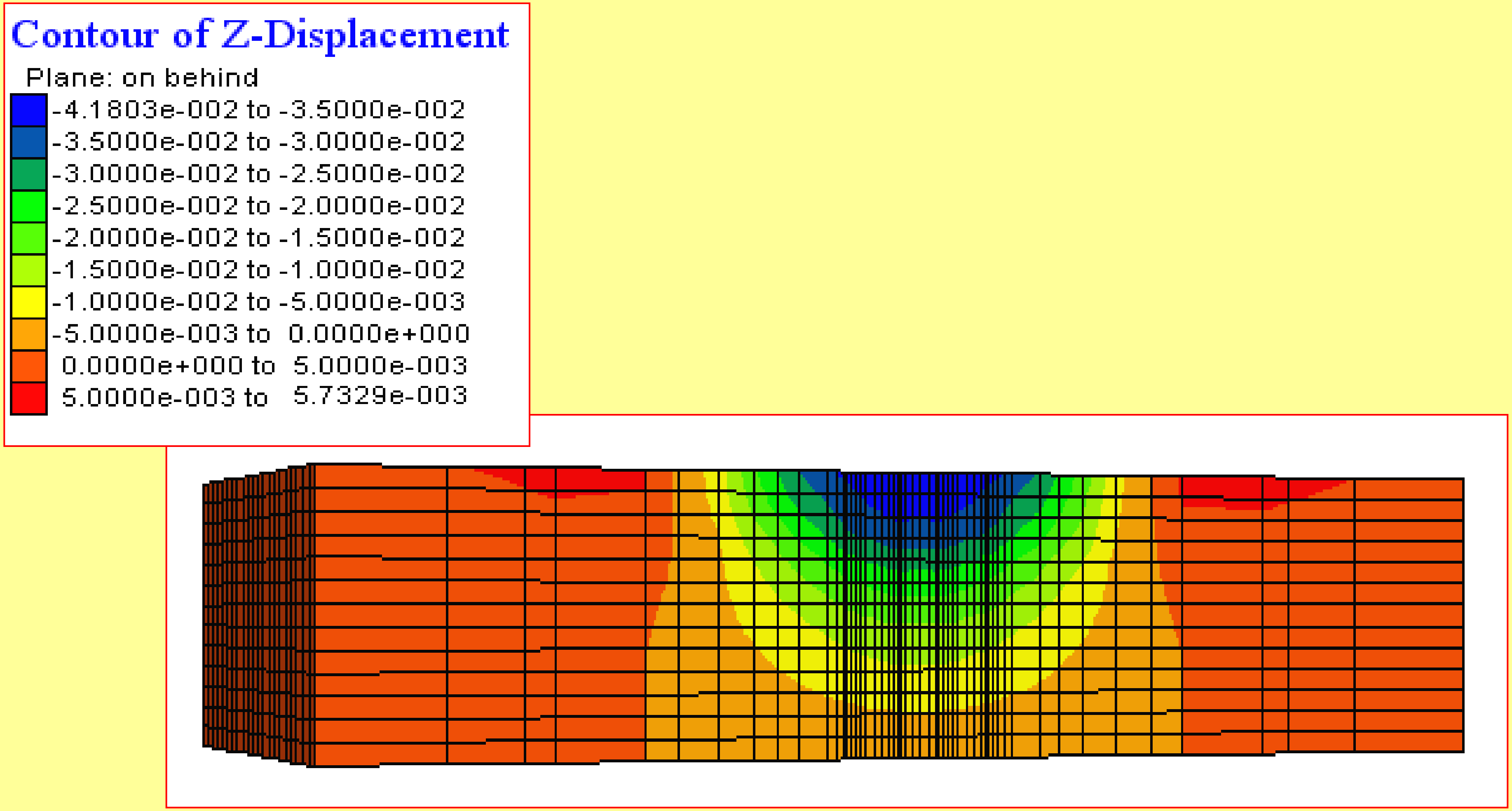

Z-Displacement (Settlement) Contours of the *DMM* Improved Ground of Wall Type at the End of Instrumentation

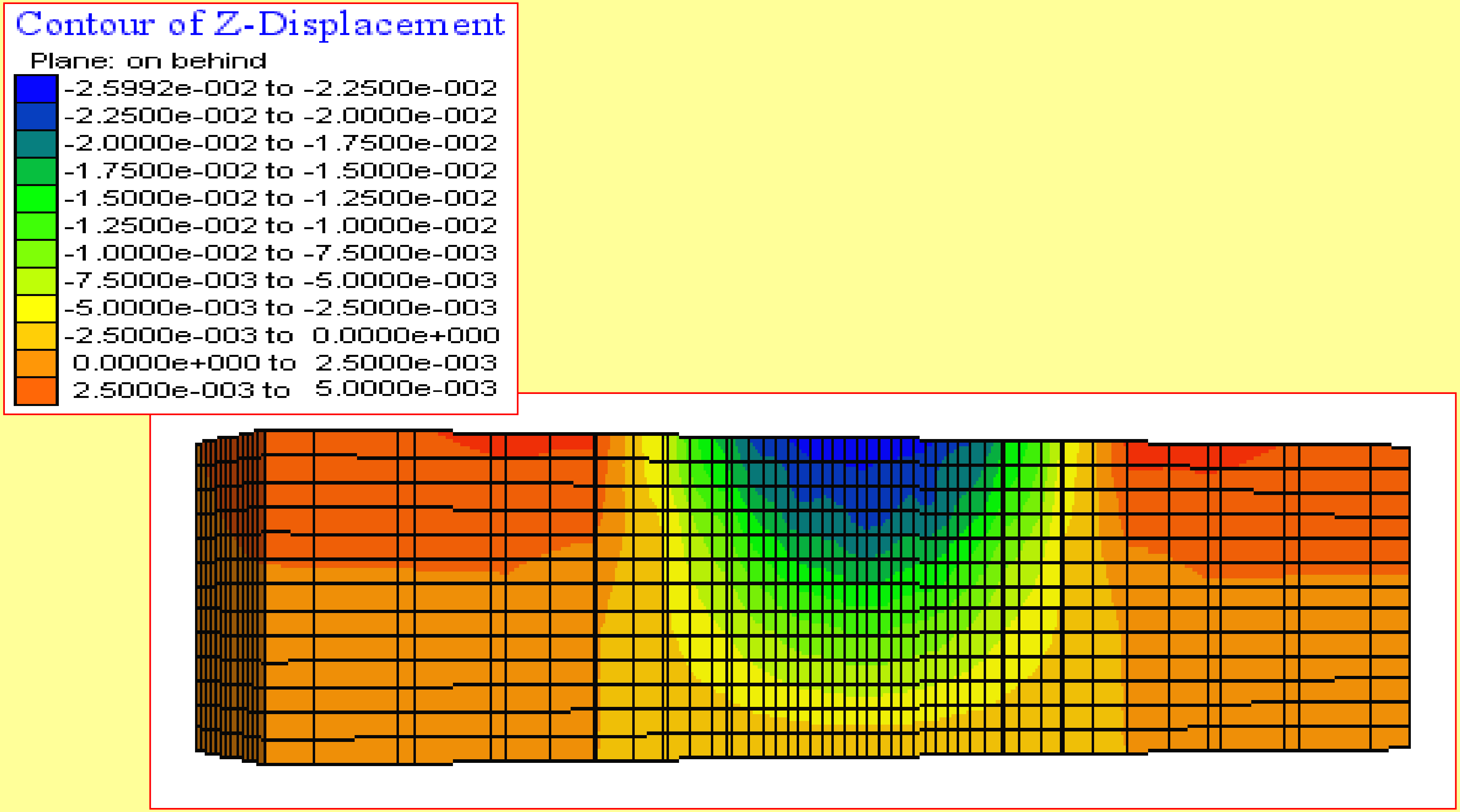

Comparison of Excess Pore Water Pressure between 3-D Numerical Prediction and Field Observation

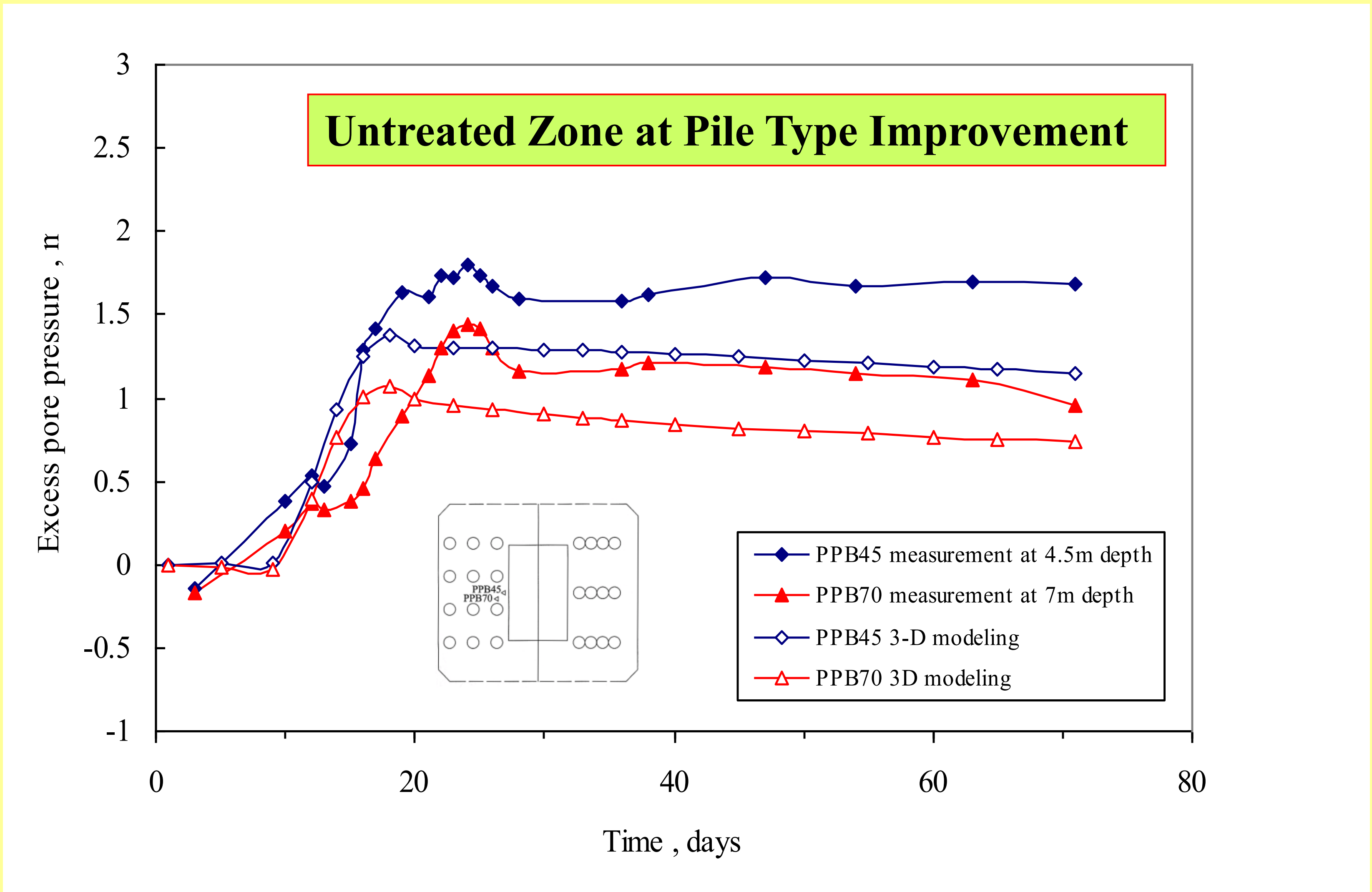

Comparison of Excess Pore Water Pressure between 3-D Numerical Prediction and Field Observation

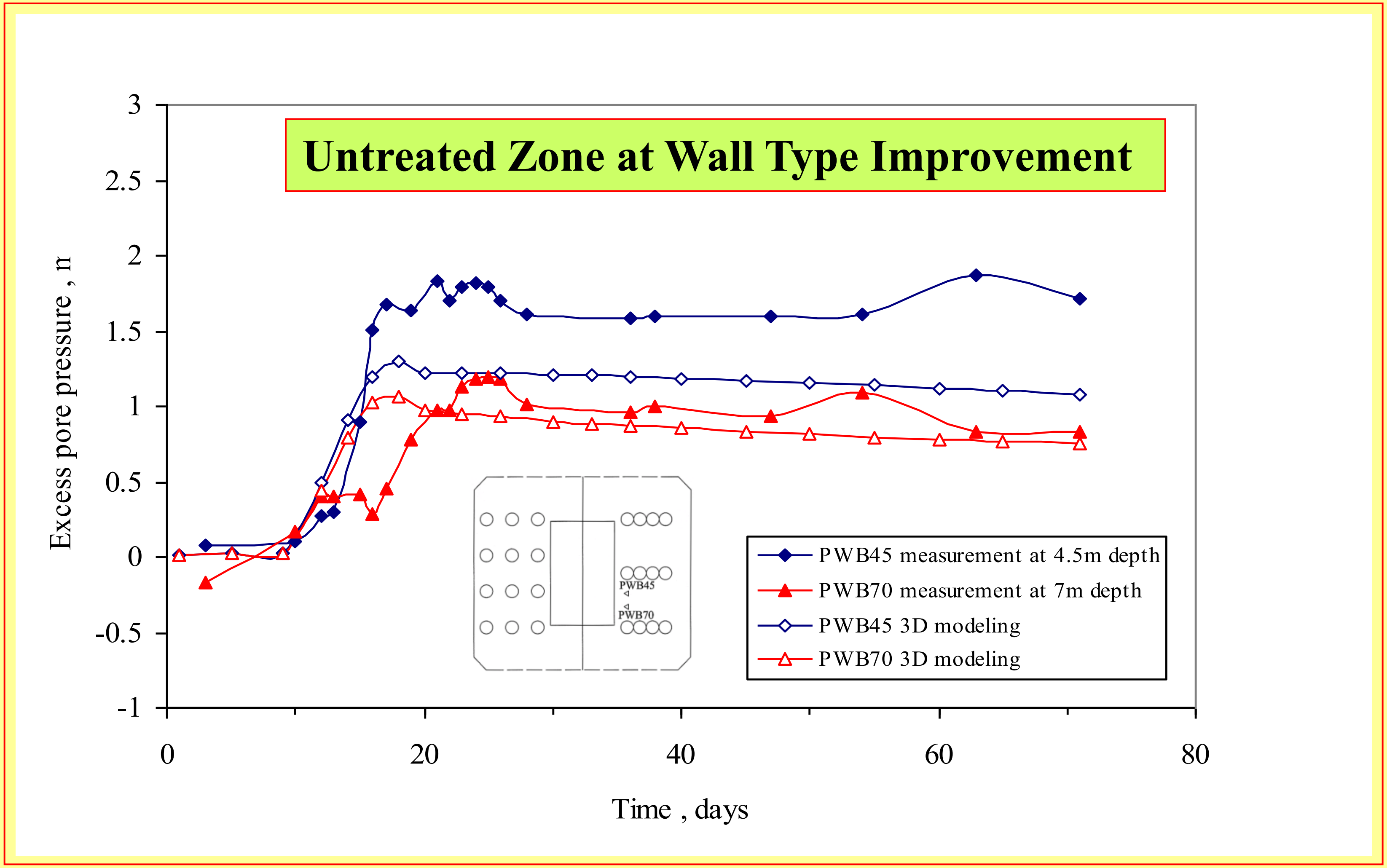

Pore Water Distribution of the *DMM* Improved Ground at the End of Instrumentation

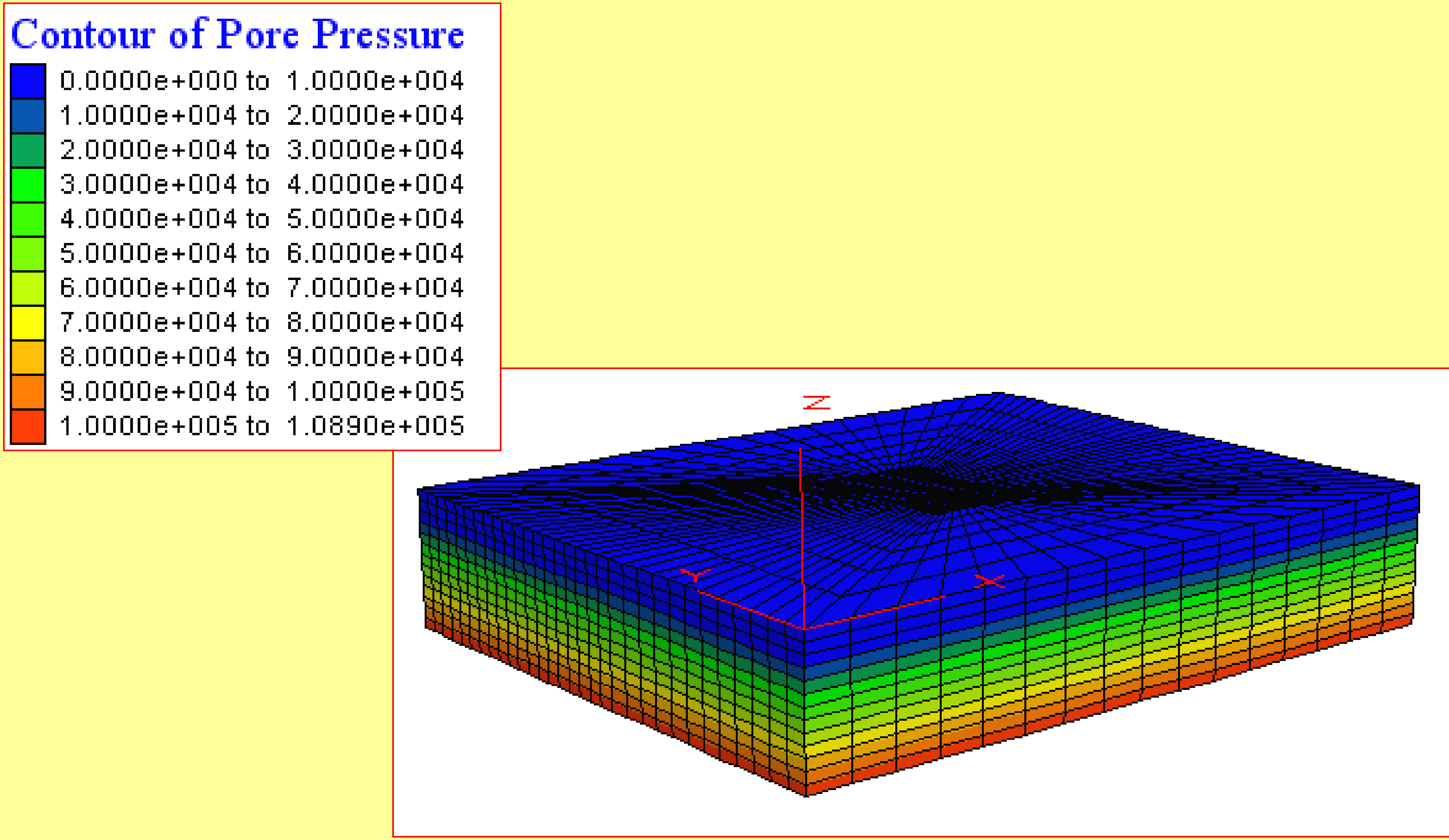

Comparison of Lateral Movement between 3-D Numerical Prediction and Field Observation for Treated and Untreated Zones

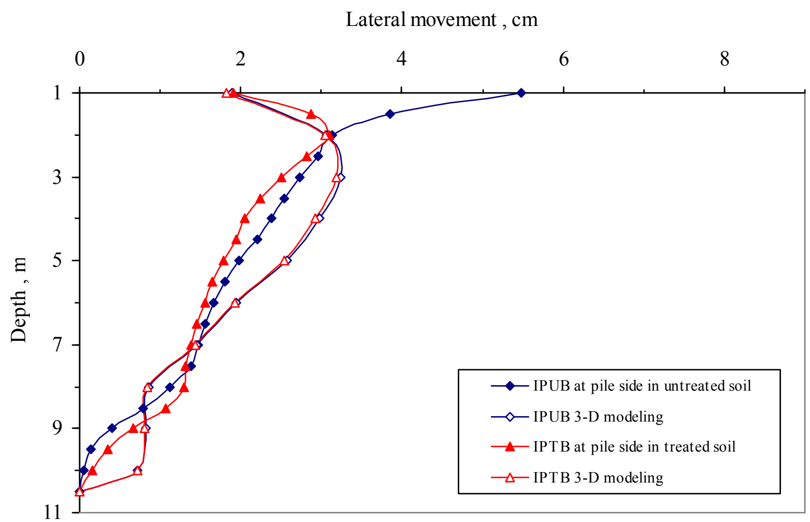

Pile Type Improvement

Wall Type Improvement

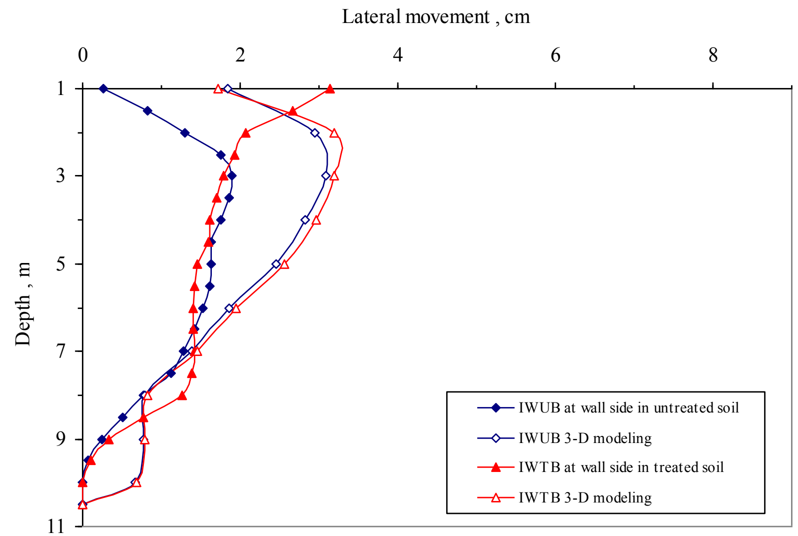

Y-Displacement (Lateral Movement) Contours of the *DMM* Improved Ground of Pile Type at the End of Instrumentation

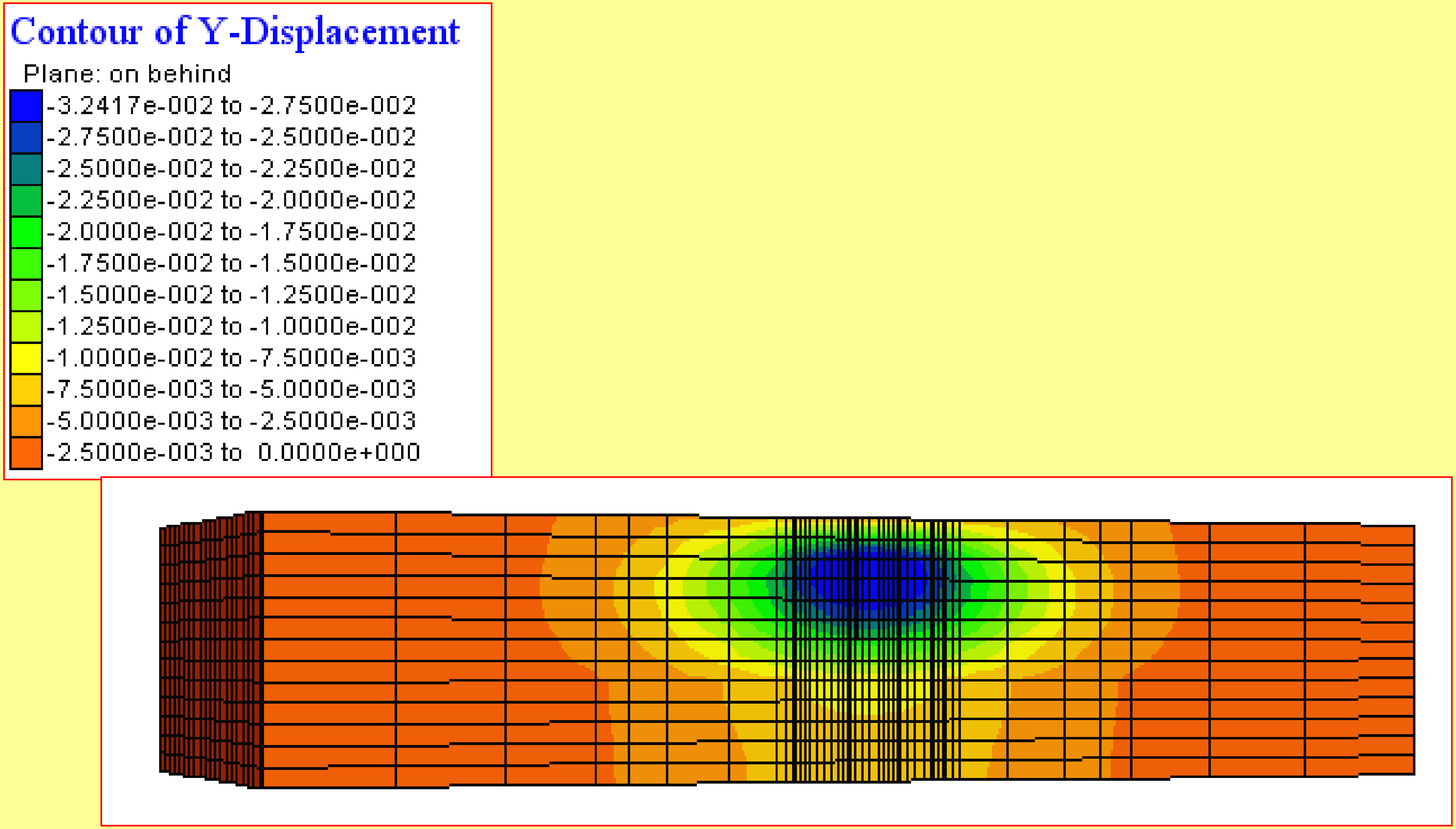

Y-Displacement (Lateral Movement) Contours of the *DMM* Improved Ground of Wall Type at the End of Instrumentation

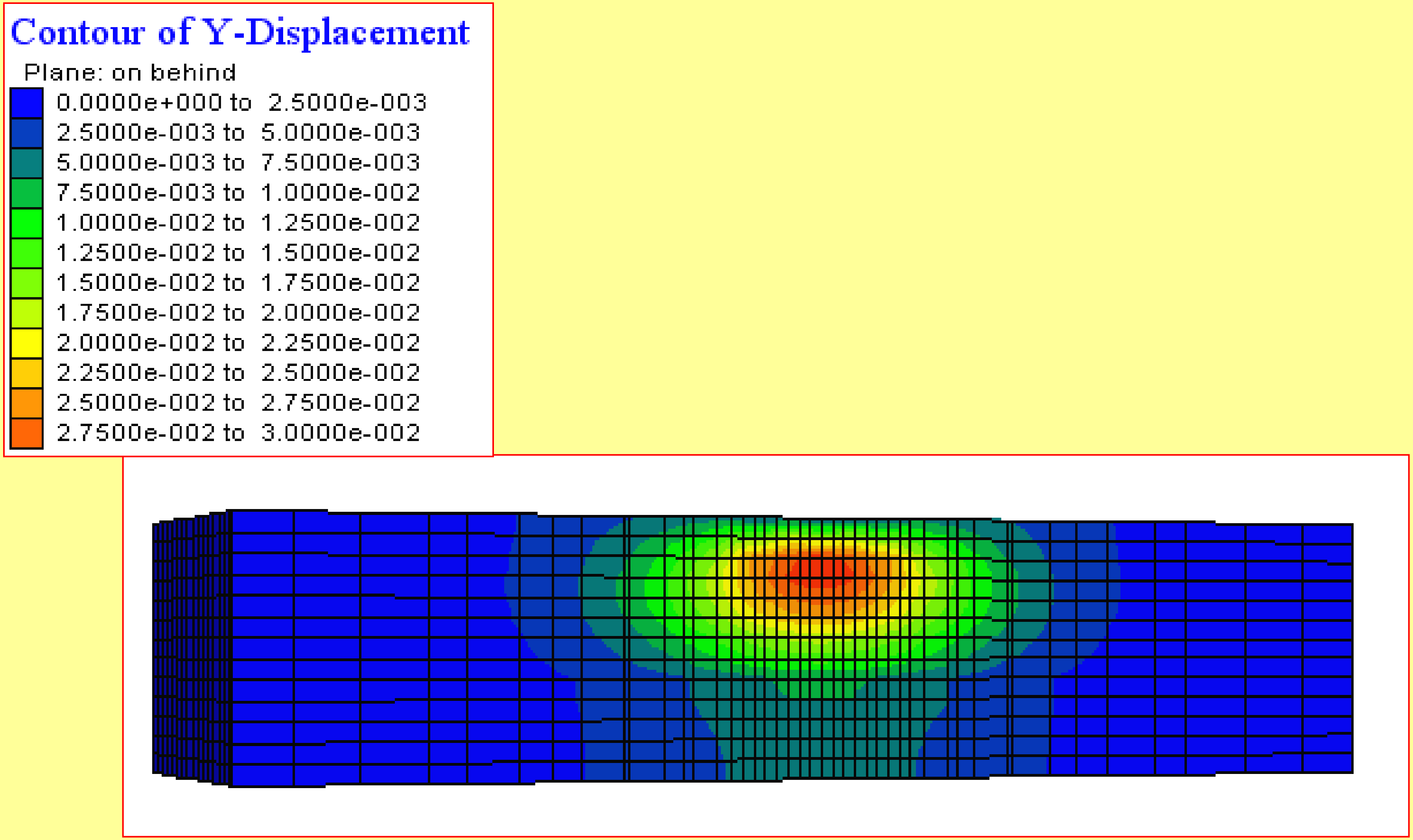

2-D Plain Strain Analysis of
Full-Scale *DMM* Improved Ground

Finite Difference Mesh for 2-D Plane Strain Analysis of *DMM* Improved Ground

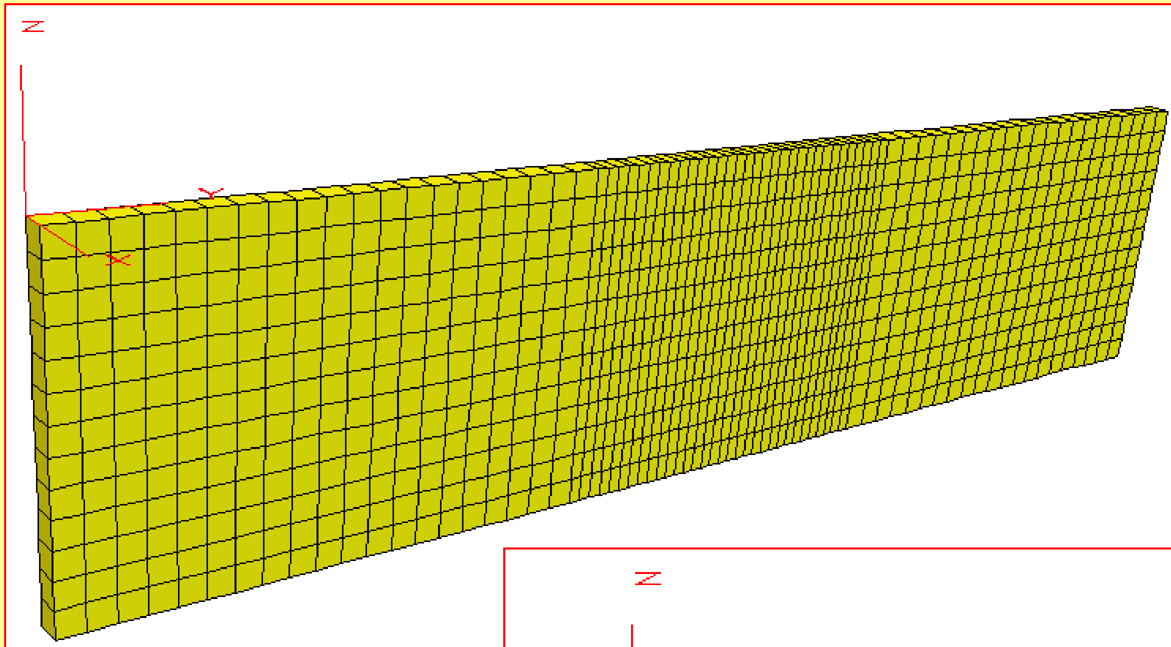

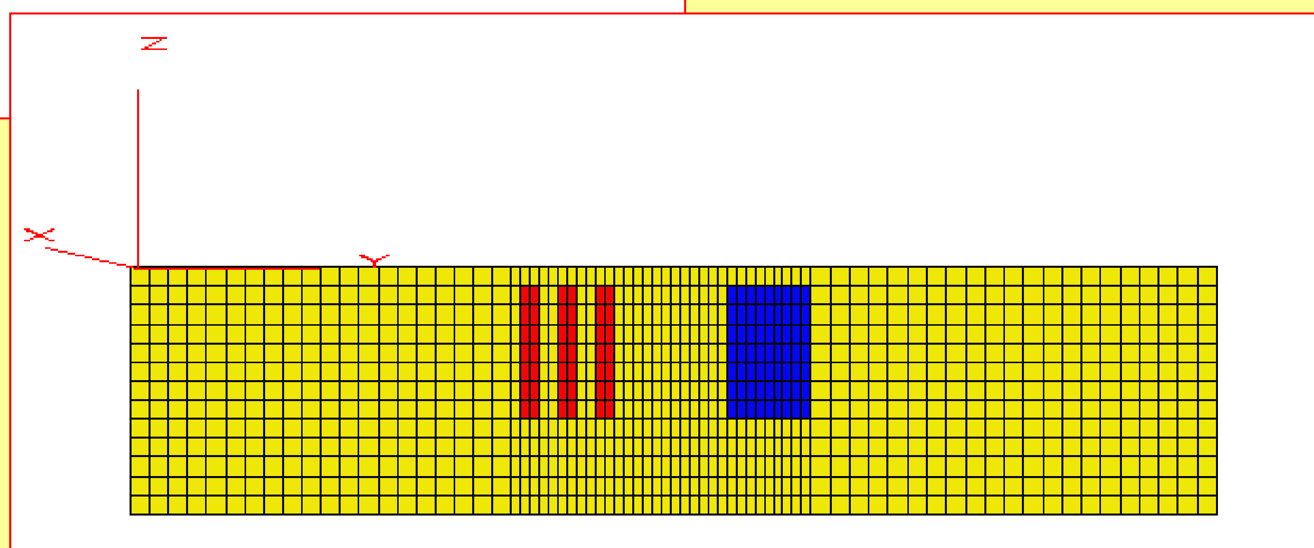

Geometry of 2-D Plain Strain Analysis of *DMM* Improved Ground

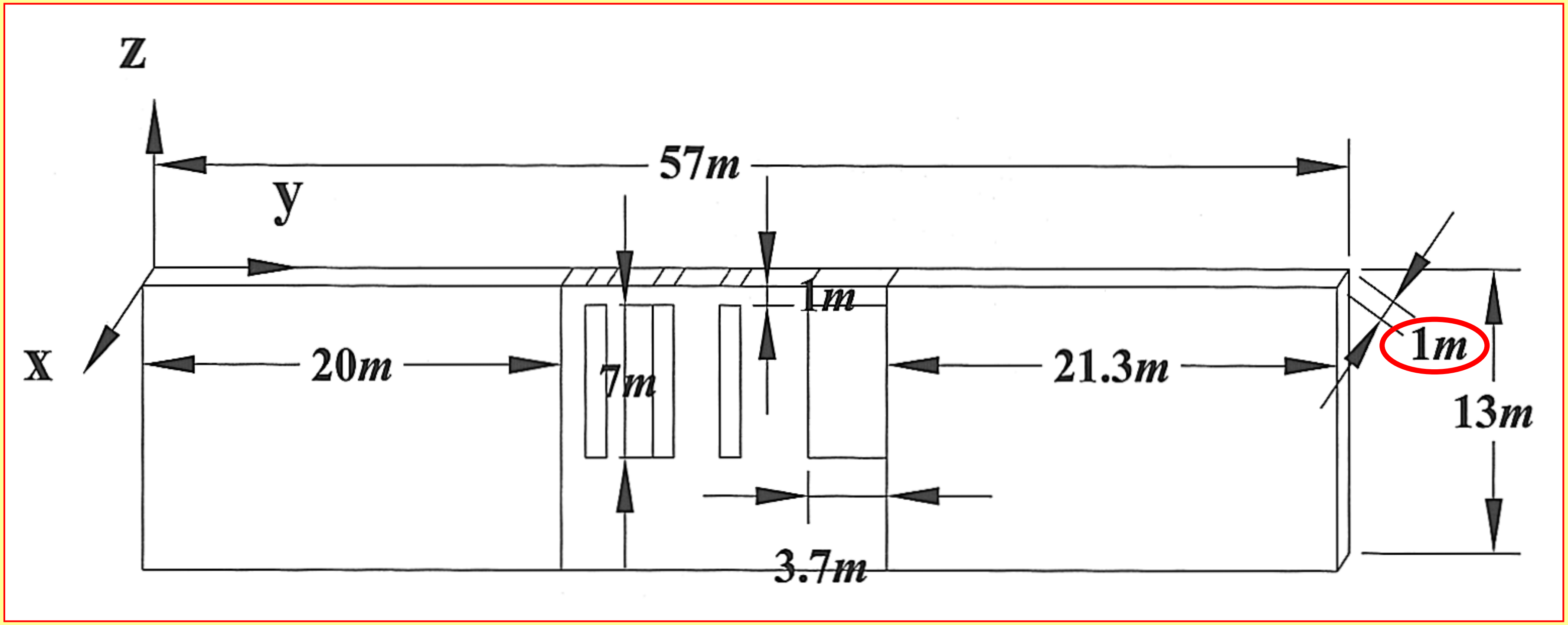

Input Parameters for 2-D Plain Strain Analysis of *DMM* Improved Ground

Depth (m)	K (x10^3 kpa)	G (x10^3 kpa)	M	λ	k	p_{c0} (x10^3 kpa)	p_1 (Pa)	υ_λ	k (cm/sec)	n
2.0-4.0	1.46	0.56	0.899	0.481	0.0962	0.109	1	8.792	1.23×10^{-7}	0.701
4.0-6.0	1.67	0.64	0.899	0.486	0.0972	0.123	1	9.022	1.62×10^{-7}	0.71
6.0-8.0	2.30	0.88	0.899	0.251	0.0502	0.125	1	5.352	9.80×10^{-8}	0.593

Input Parameters for Modified Cam-clay Model

Input Parameters for Mohr-Coulomb Model

Depth (*m*)	*K* (x10^3*kpa*)	*G* (x10^3*kpa*)	*c'* (*kPa*)	*ϕ'* (*deg.*)	σ^t (*kPa*)	*ψ* (*deg.*)	*k* (*cm/sec*)	*n*
0.0-2.0	2	1.2	30	28	56.42	0	$2.20\text{x}10^{-7}$	0.597
8.0-9.0	12.2	4.68	10	30	17.32	0	$1.50\text{x}10^{-6}$	0.35
9.0-13.0	4.67	2.8	15	28	28.21	0	$1.62\text{x}10^{-7}$	0.615
Backfill	2	1.2	30	28	56.42	0		
Pile Type	6.71	4.03	20	36	27.53	0	$2.50\text{x}10^{-8}$	0.399
Wall Type	6.21	3.73	20	36	27.53	0	$2.50\text{x}10^{-8}$	0.399

Scaled by Column Spacing, *s*

$\sigma^t = c'/\tan\phi'$ = tension limits

Comparison of Settlement between 3-D Numerical Prediction and 2-D Plain Strain Analysis for Instrumentations

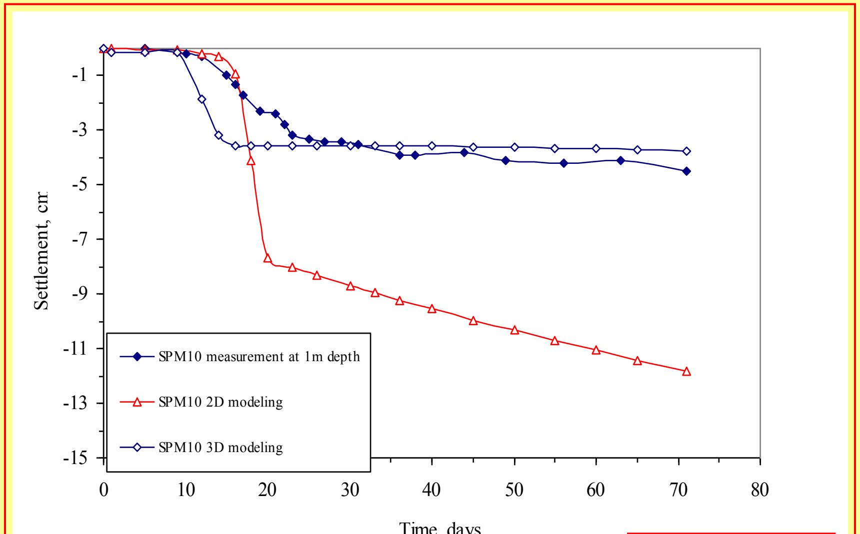

SPM10

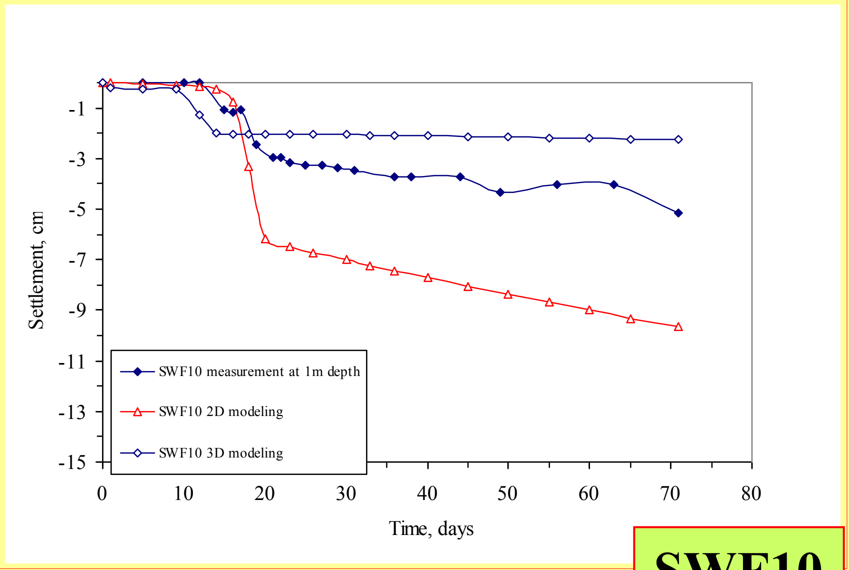

SWF10

Comparison of Settlement between 3-D Numerical Prediction and 2-D Plain Strain Analysis for Instrumentations

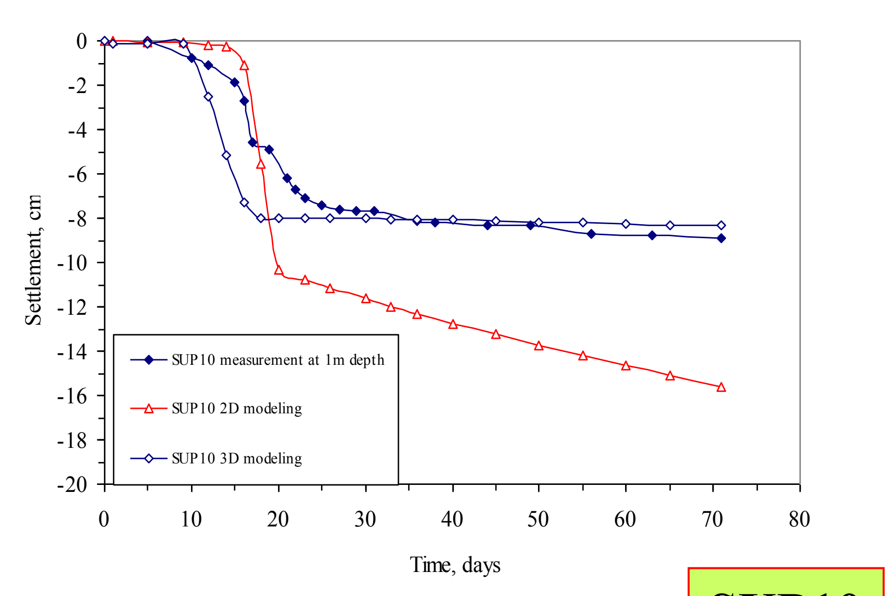

SUP10

Conclusion (1)

(**1)**According to the settlement performance of unit cell analysis, good agreement is found between the numerical results and mathematical solutions (Alamgir et al ,1996). Consequently, the effectiveness of numerical procedures is verified for *DMM* composite ground.

(**2)**For excess pore water pressure, the predicted trends were in agreement with those of the measurement. The numerical results indicate that the calculated pore pressure is sensitive to the input permeability *k* of unimproved soil.

Conclusion (2)

(3) The predicted lateral movements from analysis at the pile type improvement show good agreement with the field observation. Examining the lateral displacement and the pattern of deformation curves , it can be found that the relative movement between improved zone and unimproved zone seems not obvious.

(4) From 2-D numerical simulation, it can be concluded that the 3-D analysis is capable of revealing more realistic deformation of *DMM* improved ground than that of 2-D plane strain analysis and can give better predictions.

Recommendations

(1)To examine the interface behaviors of the improved zones and the unimproved zones at the wall type improvement in detail during and after construction of the embankment.

(2)To investigate the effects of construction parameters of *DMM* improved ground such as：(1) column diameter, *D* (2) column length, *L* and (3) column spacing, *s* and (4) configuration pattern on deformation performance.

The End

- M. Terashi and H. Tanaka (1983) presented that the treated soil behaves as elastic material with very low permeability and that soft soil consolidate one-dimensionally under decreasing loading due to gradual stress concentration to treated soil.

Location of Testing Embankment for *DMM* Improvement Ground at *AIT* Campus

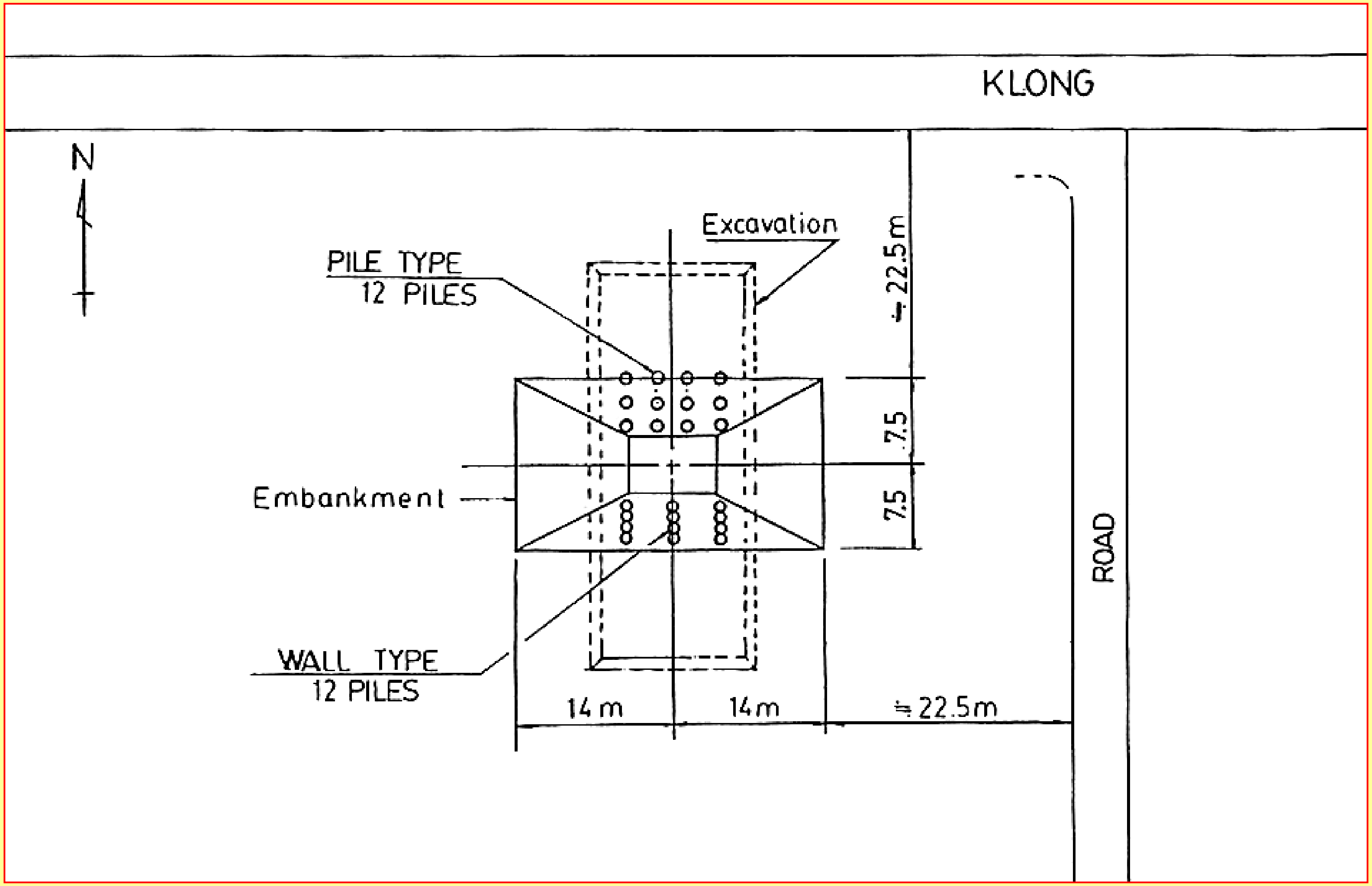

(2) For *DMM* unit cell analysis, the compressive stress in the column increases as the depth increasing while in the soil decreases with the increasing depth. It can be concluded that the relative stiffness of column and soil have significant influence on the magnitude of load transfer because the factor influence the mobilization of shear stress and the distribution of load sharing.

(2) The predicted settlement in the analysis show good agreement with the field observation. Comparison indicates that the performance of settlement could be well predicted with the proper selection of the soil parameters and material models.

Yield function: $$f(q,p) = q^2 + M^2 p(p - p_c)$$

Frictional constant: $$M = \frac{6\sin\phi'}{3 - \sin\phi'}$$

The slopes of the normal consolidation line: $$\lambda = C_c / \ln(10)$$

The slopes of the swelling lines: $$\kappa \approx C_s / \ln(10)$$

κ is usually chosen in the range of one-fifth to one-third of λ

Preconsolidation pressure:

$$q^2 = M^2[p(p_{c0} - p)]$$

$$K_{nc} = \frac{\sigma_{h\max}}{\sigma_{v\max}} \cong 1 - \sin\phi'$$

$$p_{\max} = \frac{\sigma_{v\max} + 2\sigma_{h\max}}{3}$$

$$q_{\max} = \sigma_{v\max} - \sigma_{h\max}$$

$$p_{c0} = p_{\max} + \frac{q_{\max}^2}{M^2 \times p_{\max}}$$

Initial values for specific volume:

$$\upsilon_0 = \upsilon_\lambda - \lambda \ln(\frac{p_{c0}}{p_1}) + \kappa \ln(\frac{p_{c0}}{p})$$

$$K = \frac{\upsilon_0 p_0}{\kappa}$$

$$v = \frac{3K - 2G}{6K + 2G}$$

$$G = \frac{3K(1-2v)}{2(1+v)}$$

Column Displacement:

$$\left(\sigma_{cz} + \Delta\sigma_{cz}\right)\frac{\pi d_c^{\,2}}{4} - \sigma_{cz}\frac{\pi d_c^{\,2}}{4} - \tau_{az}\pi d_c \Delta z = 0$$

$$\frac{d\sigma_{cz}}{dz} = \frac{4}{d_c}\tau_{az}$$

$$\frac{d\sigma_{cz}}{dz} = \frac{E_s\left(1-\beta_c\right)\alpha_{cz}}{a^2\left(1+\nu_s\right)}$$

$$\sigma_{cj+1} = \sigma_{cj} + \frac{\left(\Delta H/a\right)\cdot\left(1-\beta_c\right)E_s\alpha_{cj}}{a\left(1+\nu_s\right)}$$

$$w_{cj} = \frac{\Delta H}{E_c}\sigma_{cj} + \frac{\left(\Delta H/a\right)^2\left(1-\beta_c\right)E_s\alpha_{cj}}{2E_c\left(1+\nu_s\right)}$$

Soil Displacement:

$$\left(\sigma_{sNz} + \Delta\sigma_{sNz}\right)\left[\pi b^2 - \pi\left(b - \Delta r\right)^2\right] - \sigma_s N_z \left[\pi b^2 - \pi\left(b - \Delta r\right)^2\right] + \tau_{Nz} 2\pi\left(b - \Delta r\right)\Delta z = 0$$

$$\frac{d\sigma_{sNz}}{dz} = -\frac{\left(n - \Delta R\right)\tau_{Nz}}{a\Delta R\left(n - \Delta R/2\right)}$$

$$\frac{d\sigma_{sNz}}{dz} = -\frac{\left(n - \Delta R\right)\left[1 - \beta_c e^{\beta_c\left(n - \Delta R - 1\right)}\right]E_s \alpha_{cz}}{2a^2 \Delta R\left(n - \Delta R/2\right)\left(1 + \nu_s\right)}$$

$$\sigma_{sNj+1} = \sigma_{sNj} - \frac{\left(\Delta H/a\right)\left(n - \Delta R\right)\left[1 - \beta_c e^{\beta_c\left(n - \Delta R - 1\right)}\right]E_s \alpha_{cj}}{2a\Delta R\left(n - \Delta R/2\right)\left(1 + \nu_s\right)}$$

$$w_{sNj} = \frac{\Delta H}{E_s}\sigma_{sNj} - \frac{\left(\Delta H/a\right)\left(n - \Delta R\right)\left[1 - \beta_c e^{\beta_c\left(n - \Delta R - 1\right)}\right]\alpha_{cj}}{4\Delta R\left(n - \Delta R/2\right)\left(1 + \nu_s\right)}$$